Multiscale Structural Investigation of Bamboo Under Compressive Loading

by

Junhe Cui

B.Eng, Civil and Structural Engineering

City University of Hong Kong, 2016

SUBMITTED TO THE DEPARTMENT OF CIVIL & ENVIRONMENTAL ENGINEERING IN PARTIAL FULFILLMENT OF THE REQUIREMENT FOR THE DEGREE OF

MASTER OF ENGINEERING IN CIVIL AND ENVIRONMENTAL ENGINEERING

AT THE

MASSACHUSETTS INSTITUTE OF TECHNOLOGY

June 2017

Signature redacted

Signature of Author: .....

Department of Civil and Environmental Engineering

May 12, 2017

Signature redacted

Certified by: .....

Markus J. Buehler

McAfee Professor of Engineering

Professor & Department Head

Thesis Supervisor

Signature redacted

Accepted by: .....

Jesse Kroll

Associate Professor of Civil and Environmental Engineering

Associate Professor of Chemical Engineering

Chair, Graduate Program Committee

Multiscale Structural Investigation of Bamboo Under Compressive Loading

by
Junhe Cui

Submitted to the Department of Civil & Environmental Engineering on May 12, 2017 in Partial Fulfillment of the Requirement for the Degree of
MASTER OF ENGINEERING IN CIVIL AND ENVIRONMENTAL ENGINEERING
AT THE
MASSACHUSETTS INSTITUTE OF TECHNOLOGY

Abstract

Bamboo has been widely utilized as a load bearing material in building construction since ancient times by taking advantage of its excellent mechanical performance under loading as well as its low density and rapid growth. Application of bamboo to engineering, architecture and infrastructure requires in-depth understanding of the relationship between its morphology and mechanics, including how this regularly spaced segmental structure is optimized for its load bearing capability. However, our current knowledge about the linkage between the hierarchical structure and mechanical performance of bamboo is quite limited and we have little idea about the contribution of its regular spaced segment to its excellent mechanical behavior under various kinds of loading conditions. Here, we have implemented representative volume elements to our finite element analysis to study the mechanical response of the entire bamboo under compressive force and systematically investigated how the bamboo's meso-scale and macro-scale structural features (e.g., gradient fiber distribution, periodic nodes, etc.) contribute to its strength in compression. We find that column buckling is a critical failure mode that leads to overall collapse of the structure, which can be disastrous. We observe that the gradient fiber distribution pattern along the bamboo thickness direction significantly contributes to its strength. We find that the occurrence of fiber deviation at the node region reduces the strength of bamboo. Nevertheless, our results show that structural features such as external ridge and internal diaphragm play the role of reinforcement while the effect is more significant for bamboo than other plants with similar node appearance. The work reported in this thesis provides structural insights into the outstanding mechanics of bamboo, which could offer guidance for engineers to evaluate the material mechanics according to its structure and design high-performance structures with bamboo accordingly.

Thesis Supervisor: Markus J. Buehler

Title: McAfee Professor of Engineering

Acknowledgements

I would like to express my deepest gratitude and appreciation to all those who gave me assistance to complete this thesis research, both directly and indirectly. A special thanks to my thesis supervisor, Professor Markus J. Buehler, who gave me continuous guidance, encouragement, and inspiration to continue efficiently working on this research and obtain promising results. I would like to thank Dr. Zhao Qin, a research scientist in Laboratory of Atomistic and Molecular Mechanics (LAMM) for his instruction, help and innovative ideas throughout this research. I would also like to thank Professor Admir Masic, for introducing me to this amazing bamboo research.

Furthermore, I would like to thank Professor John A. Ochsendorf and Dr. Gordana Herning for making the Master of Engineering program so interesting. I benefited a lot from the challenging structural design projects. Thanks to my lovely MEng classmates and LAMM groupmates for making my master study enjoyable.

Last but not least, many thanks goes to my dearest parents and friends, for their love, understanding, encouragement, and confidence in me.

Junhe Cui
Cambridge, Massachusetts
2017

List of Contents

List of Contents

List of Contents

List of Figures

List of Figures

Chapter 6

List of Tables

Chapter 4

Chapter 5

List of Equations

Chapter 4

Chapter 1 Introduction

1.1 Background

Bamboo is a perennial plant which belongs to the subfamily *Bambusoideae* of the grass family *Poaceae* (Figure 1a) [1]. A majority of bamboo species grow in tropical and subtropical areas, where the climate is warm and moist. Owing to its unique rhizome-dependent system, bamboo is one of the fastest growing plants in nature, making it abundantly available and sustainable material [2]. In its natural habitat, bamboo acts as a cantilever beam with a fixed support in the earth and subjected to its own weight and wind load (Figure 1b), resulting in its great toughness and excellent strength to resist bending moment and compressive force [3]. The strengths are highest among the outside and lowest on the inside surfaces respectively [4]. In general, the strengths are also highest in those sections closer to the ground.

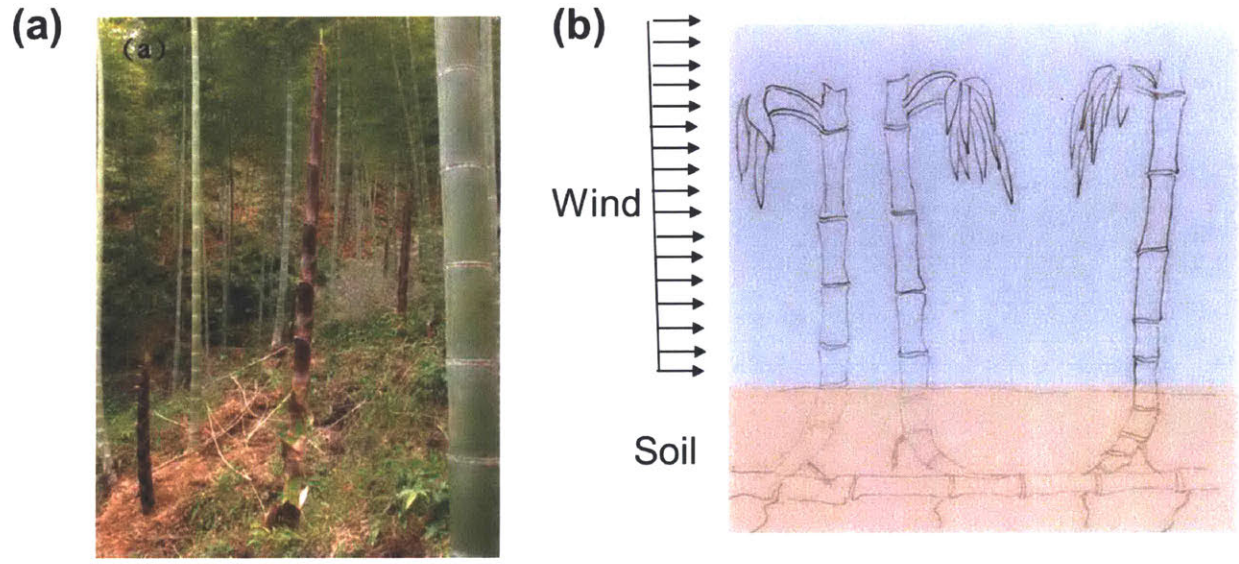

Figure 1 Bamboo in its natural habitat. (a) Bamboo forest. Reproduced with permission from Ref [5]. (b) Bamboo culm under wind load acts like a cantilever beam.

Due to its high tensile strength, excellent flexural rigidity and low density , bamboo has been widely utilized as building material for both temporary and permanent structures since ancient

times [6, 7]. Comparing with other common construction materials, bamboo has higher compressive strength than wood and concrete [8] and its tensile strength is comparable to that of rivals' steel [9]. Thus, structures made of a bamboo range from scaffolding, bridges, and houses etc. According to historical documentation, the first bamboo scaffolding was constructed 5000 years ago [10]. Nowadays, bamboo scaffolds have been widely used in a construction site in South East Asia, particularly Hong Kong and Southern China, providing the temporary access and preventing construction debris from falling onto the pedestrians [11]. In these structures, bamboo columns are exposed to compressive loading and buckling is the most critical failure mode for these members, causing the catastrophic collapse of the entire structure, which is extremely dangerous. Nevertheless, our current understanding of the buckling behavior of bamboo is quite limited, which motivates me to conduct this research to unravel the linkage between structure and buckling behavior of bamboo.

The research results could possibly make an impact in the engineering design and sustainable development. With a more comprehensive understanding of the mechanical behavior of bamboo, engineers may be inspired to find a more promising application for bamboo in a variety of fields, thereby contributing to the environmental protection and sustainability. In addition, the hierarchical structure of bamboo is a result of natural selection and evolution during the past millions of years. Grasping the idea that how this structure affects the mechanical performance of structural bamboo enables us to conduct some biomimetic design of synthetic materials or structures for enhanced mechanical properties.

1.2 Research objectives

Based on the conditions introduced in the background section, the objectives of this thesis research are listed as following:

(1) To study the structural features of bamboo at multiple length scales;

(2) To propose a computational model of bamboo accurately capturing the structural features;

(3) To investigate how these structural features affect the buckling behavior of bamboo;

(4) To offer engineers new insights towards more promising applications of bamboo in structural design;

(5) To inspire researchers to develop new synthetic materials and structures by mimicking bamboo.

1.3 Research approaches

From a review of prior studies on mechanics of bamboo, multiscale structural features of bamboo and their corresponding effects on mechanical properties of bamboo are quite well understood [9, 12]. In the mesoscale, bamboo cross section consists of bamboo fibers unevenly distributed among the surrounding matrix, forming several layers. At the macroscopic scale, bamboo culms are connected by periodic nodes, which is composed of the external ridge and internal diaphragm. All of these structural features are taken into account in the computational modeling of bamboo.

To propose the computational model of bamboo, representative volume element (RVE) method is adopted. Unit cells with different fiber proportions are constructed to measure the effective material properties, i.e. engineering constants, by finite element analysis. These properties serve as the input for the complete bamboo model with the macroscopic scale structural features on which the finite element analysis are performed to measure the critical buckling load for further analysis. The function of the structural features on the buckling behavior of bamboo is investigated by comparing the critical buckling loads of these models.

1.4 Thesis organization

The thesis consists of nine chapters, with content as outlined below.

Chapter 1 Introduction

This chapter presents the general picture of this research project, including the brief introduction of the background information, motivation, and objectives of the research.

Chapter 2 Previous research on bamboo

This chapter reviews the intensive studies on the multiscale structural features of bamboo, excellent mechanical properties of bamboo from experimental results, the relationship between these features on the mechanical properties of bamboo.

Chapter 3 Finite element method

This chapter reviews the algorithms, equations, and applications of finite element method.

Chapter 4 Methodology

This chapter firstly describes the bamboo computational model development process and then explains the theoretical calculation procedure and details of the finite element analysis on bamboo models.

Chapter 5 Results

This chapter presents the result of the effect of gradient fiber distribution, the critical buckling load and the contribution of structural features.

Chapter 6 Discussions

This chapter discusses the similar features in other species and potential application of the research results.

Chapter 7 Conclusions

This chapter summarizes the key findings of the research and points out some possible directions for future research.

Chapter 1 Introduction

Chapter 8 References

Chapter 2 Previous Research on Bamboo

2.1 General information of bamboo

2.1.1 Growth of bamboo

As a species of the grass family, bamboo is a colony plant, which expands the root structure and produces more plant utilizing the energy generated by its existing plant above the ground. 80% of the mass of this colony is buried underground while the culms provide nutrients by photosynthesis for the underground colony of rhizomes, which are roots with a similar appearance of the culms in appearance [13]. Both the roots and culm have nodes and internode segments. Rhizomes are located at the nodes, which facilitate the storage of nutrients and trigger the growth of the plant. In spring season, new culms emerge out of the ground and grow in height and diameter at an amazing rate for about 60 days [14]. By observation, a bamboo could increase almost four feet in a 24-hour time during the growth period [15]. Meanwhile, the limbs and leaves are also produced. Once the new shoot reaches its maximum height, the branches and new leaves are unfolded, revealing the completion of growth period and the maturity of the cane. Afterwards, there will never be an increase in diameter or height. Generally speaking, a matured bamboo is expected to survive for about 10-15 years relying on the species.

2.1.2 Multiscale Structural features

The structure of the upper ground portion of bamboo, the bamboo cane, is of interest since it is the usable part. The bamboo is a functionally gradient structure and bamboo cane has various structural features from macroscale, mesoscale to nanoscale.

2.1.2.1 Macroscale structures

In the macroscale, the bamboo cane is a hollow culm structure, which is composed of a series of regularly spaced nodes and segments as is shown in Figure 2a. The node which supports the culm to prevent failure from local buckling, is characterized by an internal diaphragm and external ridge [16]. Unlike the straight fiber orientation along the culm, bamboo fibers start to change the orientation in the vicinity of the node and deviate from their longitudinal orientations (Figure 2b)

[17]. From a mechanical point of view, the node supports the culm to prevent failure from local buckling while from the biological point of view, the node provides a place for branches and leaves to grow, helping the nodes to generate nutrients [18]. The segment length, defined as the distance between each node, varies along the height of the culm [19]. Figure 3 shows that the value increases from the base of the culm towards somewhere below the middle, and then decreases till the top of the culm.

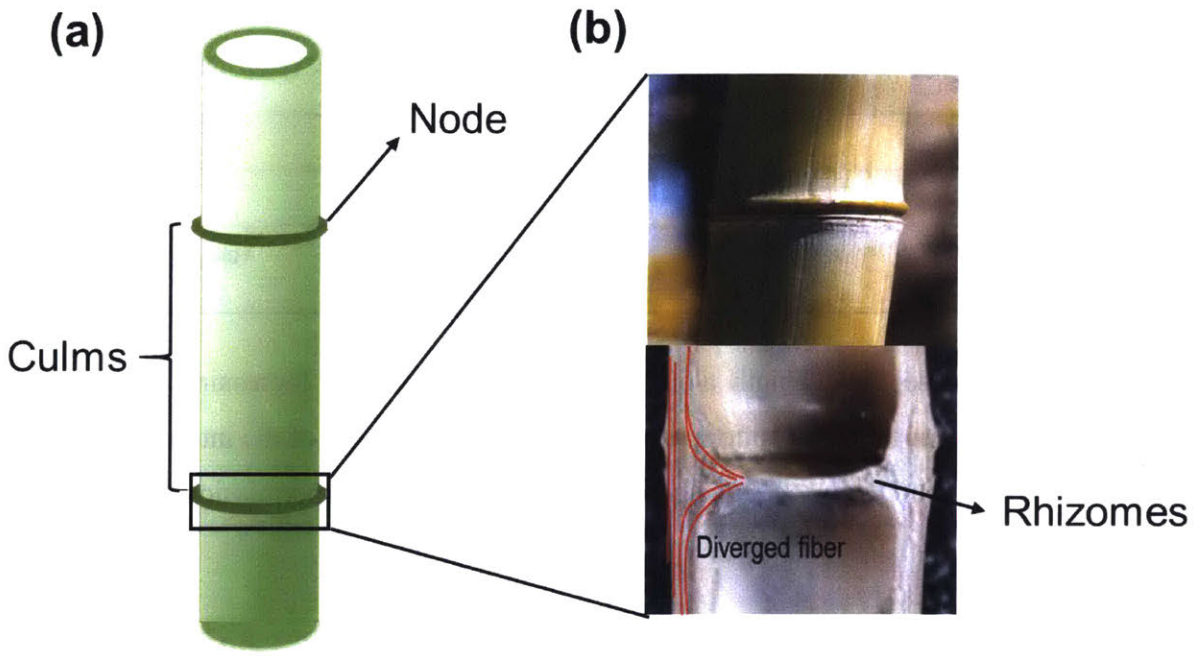

Figure 2 Macroscale structural features of bamboo. (a) Bamboo culm structure. (b) Structure of the node. Reproduced with permission from Ref [17].

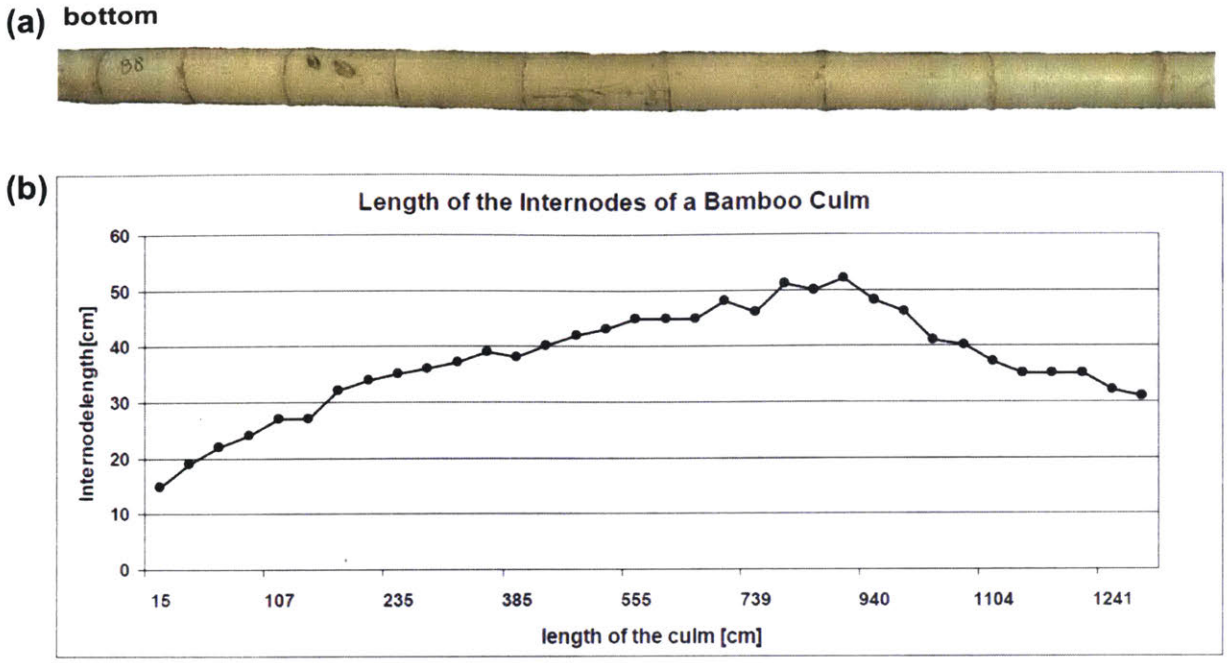

Figure 3 Variation of segment length along the bamboo height. (a) Increasing length of the internodes along the culm from the bottom part upwards. (b) The length of the internodes over the height for a giant bamboo *Dendrocalamus giganteus*. Reproduced with permission from Ref [19].

2.1.2.2 Mesoscale structures

In the mesoscale, a gradient fiber distribution is also observed along the radial direction of the bamboo cross section (Figure 4b). The volume fraction of bamboo fibers increases from the outside to the inside surface across the thickness of the bamboo culm [3]. Based on the fiber population, the thickness of bamboo cross section can be approximately classified into three regions as: (a) high fiber density (at and near the outside surface); (b) low fiber density (at and near inside surface); (c) medium fiber density (in the middle between high and low fiber density regions). In general, the fiber density ranges from 20% to 60% of the cross-sectional area along the thickness direction from the quantitative study and the average fiber density is approximately 40%. Thus, the fiber density of the three regions could be very reasonably estimated as 20%, 40% and 60% respectively.

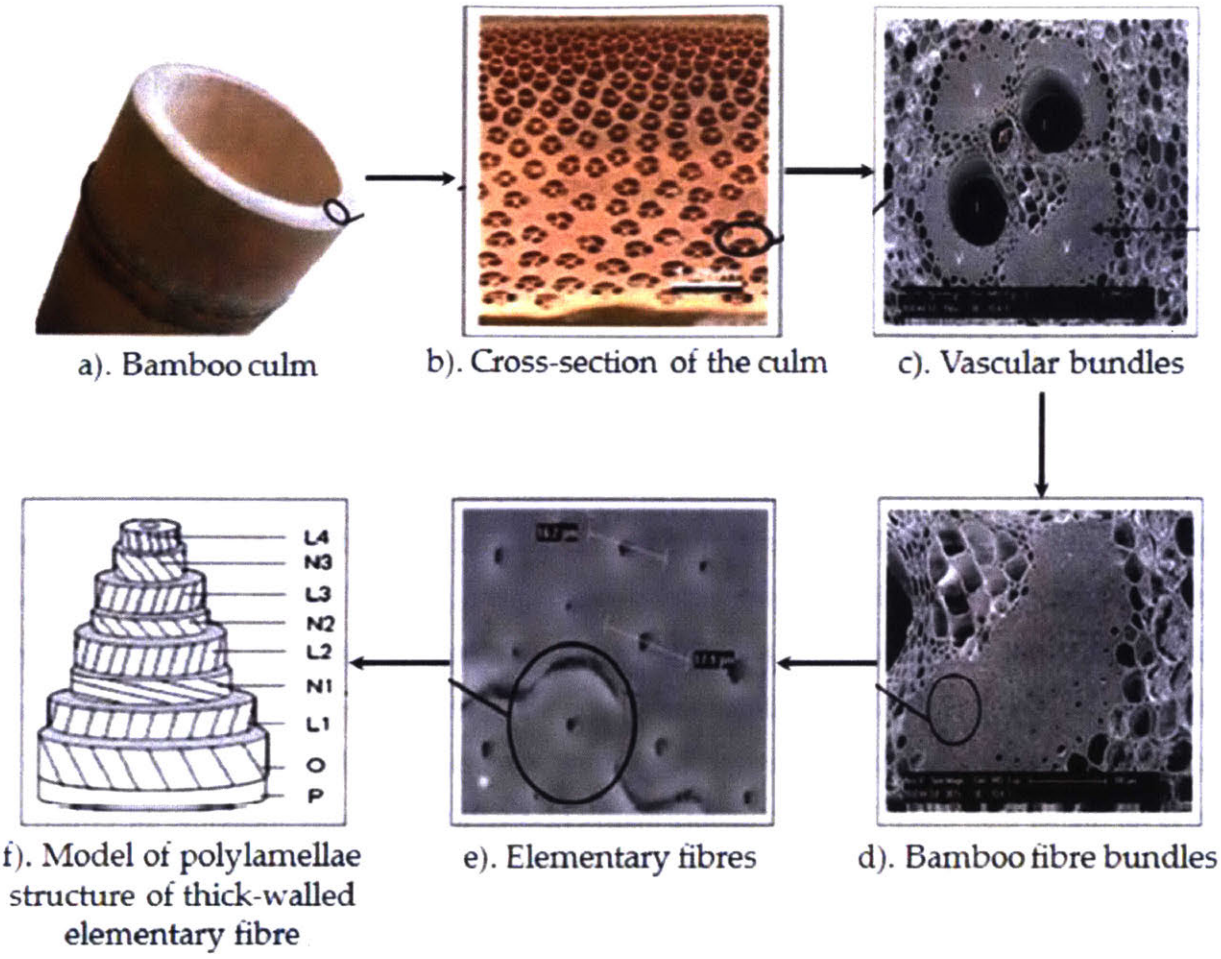

Figure 4 Visualization of the hierarchical structure of bamboo. Reproduced with permission from Ref [20].

2.1.2.3 Nanoscale structures

On the nanoscale, bamboo fibers act as fiber caps or sheaths by distributing around the conducting elements, namely vessels, sieve tubes and companion cells. These components form the vascular bundle (Figure 4c). Along the longitudinal direction of bamboo culm, bamboo fiber bundles consist of intercalated bamboo fibers with tapering at both ends (Figure 4d). These elementary fibers with the diameter of approximately 5-20 um are composed of bamboo cell walls which demonstrating a multilayered structure with 3-4 lamellae and a lumen at the center (Figure 4e and 4f). Each layer is 5-7 um in thickness and it consists bundles of the cellulose microfibrils [21]. These microfibrils are surrounded by lignin-carbohydrate complex (LCC) matrix, which contains

lignin and hemicellulose [22]. The cellulose, hemicellulose and lignin take the percentage of 73.83%, 12.49% and 10.50% distinctively [22]. Linear chains of cellulose with orderly hydrogen bonds form the crystalline regions of microfibrils while irregular hydrogen bonds create amorphous regions. The cross section of these microfibrils is either rectangular or hexagonal.

2.1.3 Mechanical behavior

2.1.3.1 Gradient mechanical properties

Bamboo has excellent mechanical properties, such as high yield strength, high toughness and light weight. Figure 5 is the Ashby plot showing the value range of bamboo's tensile strength and fracture toughness. The mechanical properties demonstrate a gradient pattern along the bamboo thickness direction. Nanoindentation tests were performed along bamboo cross-section to measure its Young's modulus [3]. It was found that the Young's modulus decreases with increasing radial distance from the outer surface. Moreover, the Young's modulus for the bamboo fibers (40 – 55 GPa) is far higher than that of the surrounding matrix (2-5 GPa). Averagely speaking, the effective elastic modulus at different regions range from 13.8 GPa to 6.7 GPa, which is consistent with the fiber density distribution mentioned before. In addition, micro-tensile tests were conducted on the dog-bone shaped bamboo specimens. Similar to the trend of Young's modulus, the ultimate tensile strength also displays a degradation corresponds to the fiber density degradation. The lowest tensile strength (210 MPa) occurs at the innermost region with the lowest fiber density while the highest strength (690 MPa) corresponds to the outermost region.

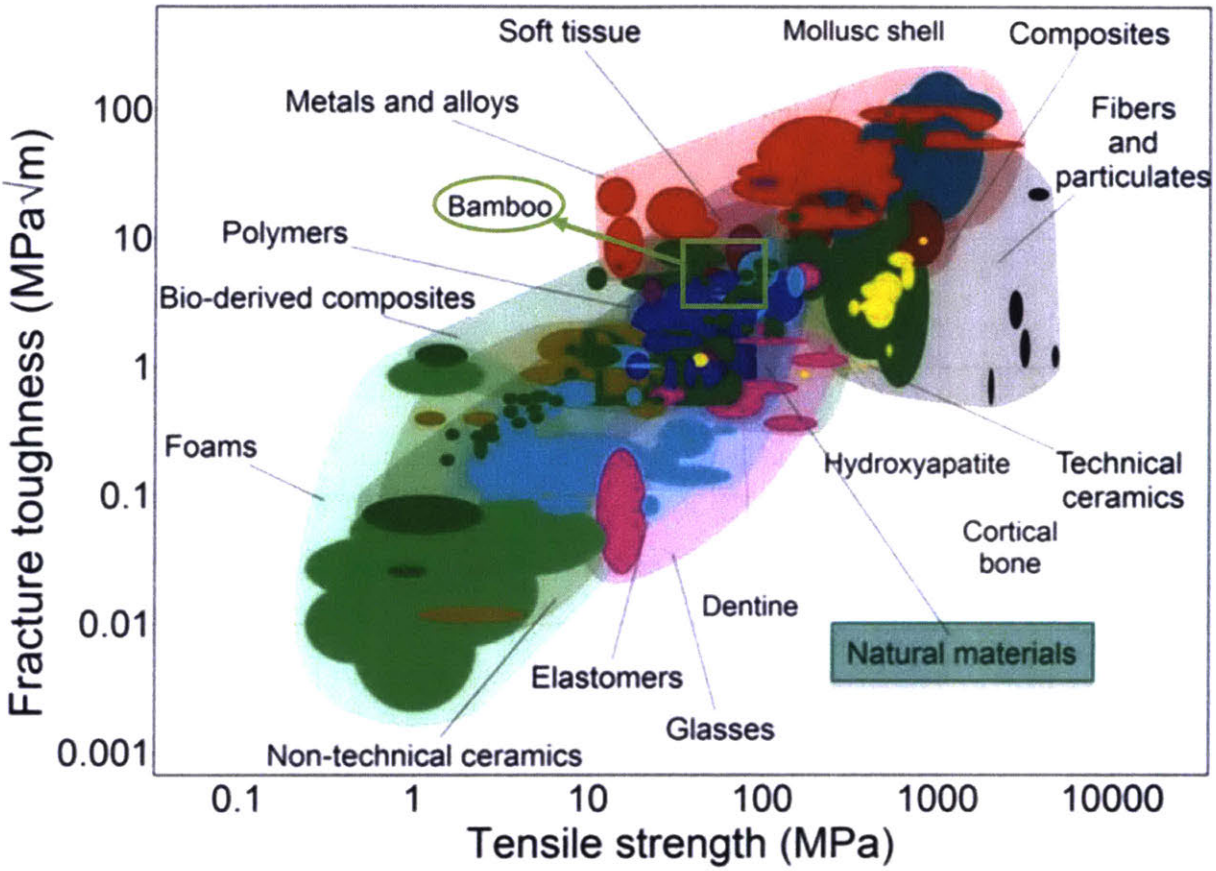

Figure 5 Ashby plot showing fracture toughness over strength relationships for various engineering materials. The bamboo region is highlighted in light green. Bamboo demonstrates high tensile strength and fracture toughness, which are roughly comparable to metals and other composite materials. Reproduced with permission from Ref [23].

2.1.3.2 Fracture behavior

Four-point bending tests were carried out on notched specimens to determine the resistance curve behavior of bamboo. It was noticed that the notch-induced crack growth occurs by deflection into the interlaminar boundaries within individualized plies [24]. In addition, mixed mode interfacial crack growth occurs with a high incidence of cellulose bridging in the outside and inside crack orientations [24]. By contrast, crack growth occurs with a significant incidence of ligament or lignin/cellulose composite bridging in the side crack orientation. The stronger outside regions with higher fiber densities result in lower levels of crack tip shielding with a lower incidence of cellulose

crack bridging. However, the weaker inside regions with lower fiber densities result in higher levels of crack tip shielding with a higher incidence of cellulose crack bridging. Intermediate toughening and resistance curve behavior is associated with crack growth in the side orientation, where crack tip shielding occurs via ligament bridging [3].

2.1.3.3 Bending behavior

Three-point and four-point bending tests were performed on bamboo specimens. The results showed that in the macroscale, a bamboo beam is a very flexible structure when its stiff outer layer was in tension while the softer inner layer was in compression. Nevertheless, the flexibility of the local parts of bamboo in the mesoscale was not as excellent as predicted. Hence, the excellent flexural ductility of split bamboo culm should be attributed to the combination of high fiber density outer part and the low fiber density inner part which is compressible [25].

2.1.4 Applications of bamboo

Bamboo has been widely utilized since ancient times and people give bamboo various kinds of applications in different industries.

2.1.4.1 Construction

As previously mentioned, bamboo has excellent mechanical properties. Its compressive strength is comparable with concrete and its tensile strength is almost 3-4 times of that of steel. More importantly, bamboo is a very light weight material and is easy to assemble on site. Due to these reasons, bamboo has been widely used to build scaffoldings, temporary structures and permanent structures (Figure 6) in construction industry. Bamboo scaffolds has been adopted on construction site in Hong Kong and Southern China after the first bamboo scaffold was built 5000 years ago [26]. Then about 2000 years ago, people have empirically established some basic framing systems and the erection methods [27]. Nowadays, scaffolds that are commonly erected are named as Double Layered Bamboo Scaffolds (DLBS) [28]. In these structures, bamboo culms act as the primary load carrying members. The advantages of bamboo scaffold over steel scaffold are its quick installation and easy handling without machinery or power-driven tools.

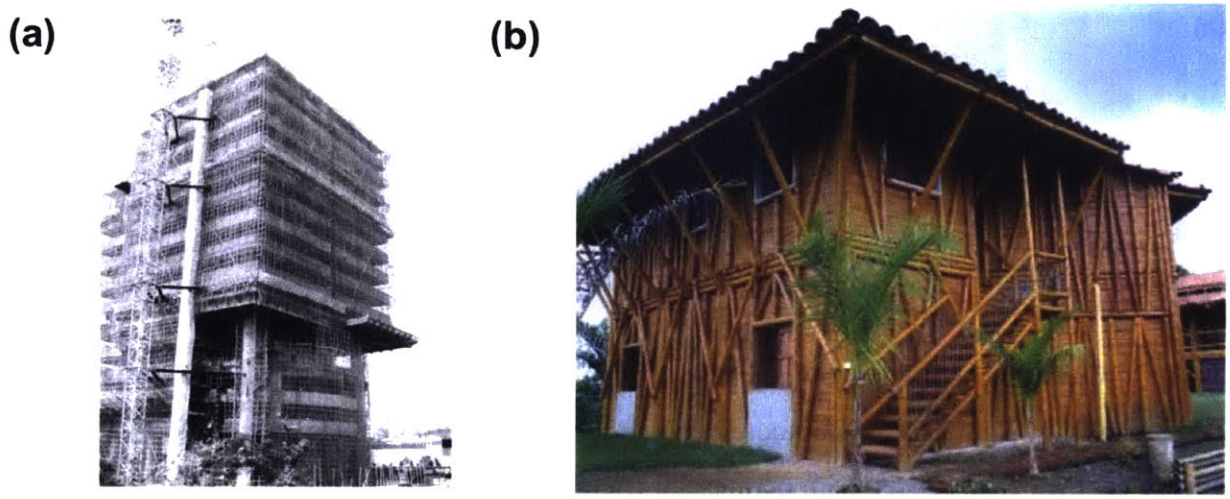

Figure 6 Photos of structures fabricated with bamboo. (a) Temporary bamboo scaffolding used for the construction of a high-rise building in Hong Kong. Reproduced with permission from Ref [12]. (b) Permanent architecture constructed with bamboo. Reproduced with permission from [29].

2.1.4.2 Furniture

Because of bamboo's easy formability, excellent mechanical properties, and non-toxicity, it is a popular and suitable material for furniture making [30]. It is very convenient to split or bend bamboo so that we can achieve various kinds of furniture. Common furniture made of bamboo (Figure 7) ranges from floor, chairs and cabinets, which can also be fabricated with wood. The replacement of wood with bamboo contributes to the preservation of forest and sustainable development.

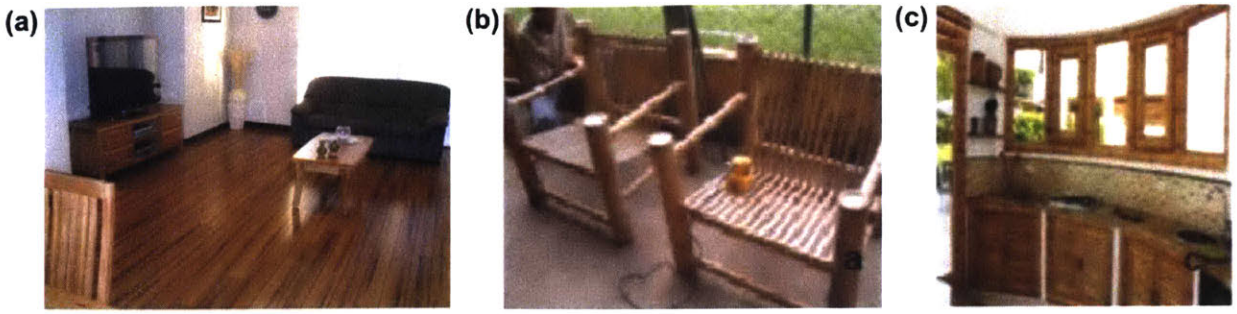

Figure 7 Common furniture pieces made of bamboo. (a) Bamboo flooring. Reproduced with permission from Ref [31]. (b) Bamboo chairs. Reproduced with permission from Ref [32]. (c) A bamboo cabinet. Reproduced with permission from Ref [32].

2.1.4.3 Musical instrument

Bamboo spans a large range in density and Young's modulus and overlaps with the requirement for many kinds of applications so it is a traditional material for musical instruments all over the world. Bamboo is well suited for different musical instrument due to its excellent physical, mechanical and acoustical properties. [33]. Common types of musical instruments fabricated with bamboo include wind instrument (aerophones), resonators and strings (Figure 8) [33].

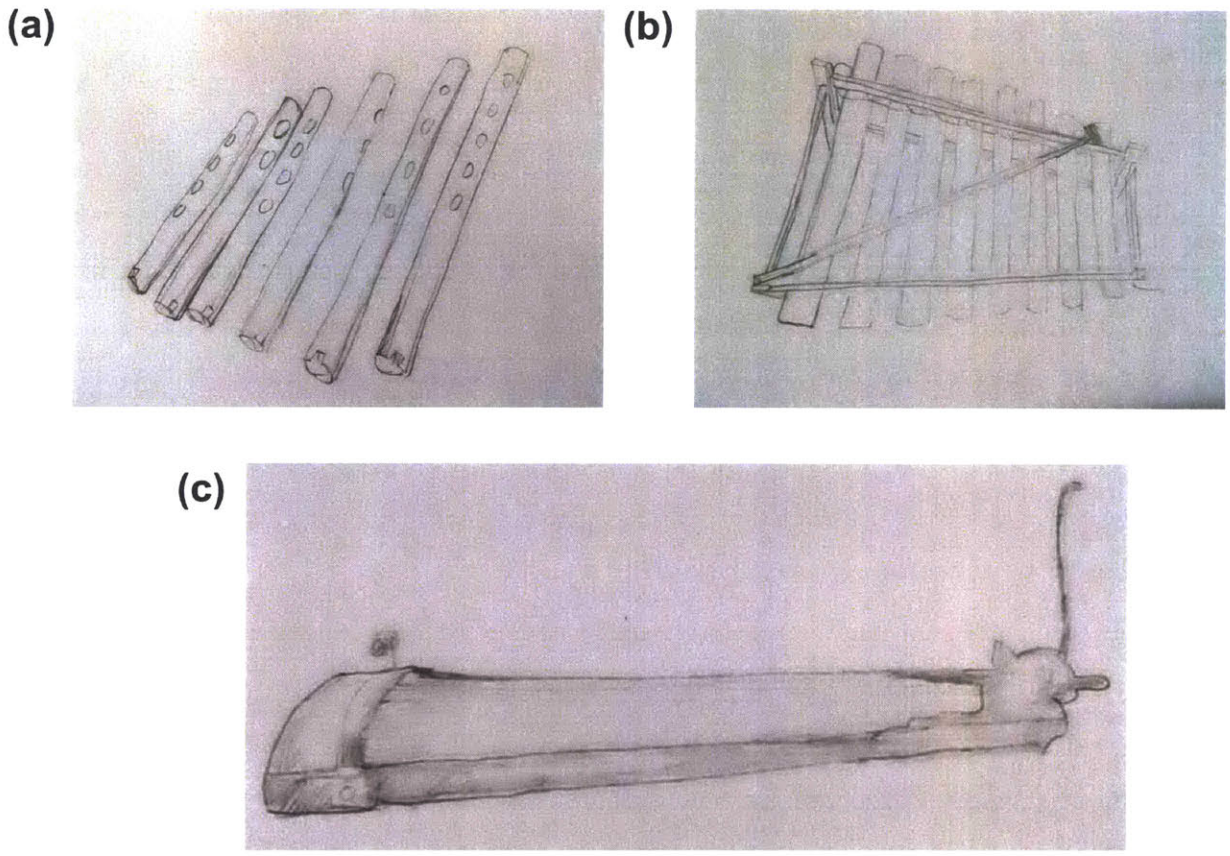

Figure 8 Examples for bamboo musical instruments [29]. (a) Bamboo aerophone. (b) Bamboo resonator. (c) Bamboo string.

2.2 Buckling of bamboo columns

2.2.1 Axial compression test on bamboo column

Axial loading tests were carried out on long bamboo columns to investigate its buckling behavior. In these tests, the slenderness ratios are taken into account by choosing columns with the length of 8.0m and 5.0m respectively. The specimen was pin connected at both ends and we record the value of axial load P and corresponding horizontal displacements for analysis. It was noted that buckling is the most dominated failure mode, indicating the demand for careful design against the buckling failure of bamboo column [34].

2.2.2 Design procedure against buckling

A bamboo column design method was proposed based on the buckling design procedure in the European Timber Code (Eurocode 5) [35] and European Steel Code (Eurocode 3) [36]. In this method, the design formulation adopts the Perry-Robertson interaction formula in order to evaluate the compressive buckling strength. The values of both the Perry factor and the Robertson constant in the formulation were chosen in according with the test data. The elastic modulus for the entire member length was chosen as the average value from the tests. The cross section properties, including the area, moment of inertia and radius of gyration were evaluated to determine the buckling strength. In addition, bamboo is a natural heterogeneous material, a non-prismatic parameter β was incorporated with the elastic Euler buckling load for the bamboo columns to consider the variation of moment of inertia along the member length [34]. In this way, the evaluated buckling strength can be used for design compressive member using bamboo.

2.2.3 Remarks on the design method

Though the design method aforementioned takes into account of the variation of diameter and thickness throughout the height of the bamboo column, it does not incorporate the macroscopic structural features of periodic nodes in the design. Moreover, the elastic modulus uses an average value and it is not accurately calculated according to the fiber distribution pattern. These assumptions are very rough because the effect of non-uniform fiber distribution and function of structural features like the internal diaphragm and external ridge are not studied. Therefore, the

proposed design method still has much room for improvement. A more comprehensive and accurate method may be produced by taking account of these features.

Chapter 3 Finite Element Method

3.1 Introduction

As the fast advancement of modern technology, engineers are facing challenges from more complex and costly projects, which are subject to severe reliability and safety constrains. In order to get a comprehensive understanding of these problems, mathematical models which allow the analyst to simulate the behavior of complex physical systems are in desperate need, thereby resulting in the emergence of finite element method (FEM). The finite element method consists of using a simple approximation of unknown variables to transform partial differential equations into algebraic equations [37].

In 1956, the concept of finite elements was created by Turner, Clough, Martin and Topp. They represented an elastic two-dimensional domain by an assembly of triangular panels across which displacements are presumed to vary in a linear manner [38]. The behavior of each panel is represented by an elementary stiffness matrix. Structural mechanics tools are then employed to obtain nodal displacements under different applied loads and boundary conditions.

Later on, finite element method was recognized as a general method of solution for partial differential equations [39]. It thus came into use in solving non-linear and transient problems of structures. Nowadays, finite element method is widely used in industrial applications, including aerospace, automobile, and structural engineering [38]. A number of commercial software has been developed over the years, such as ABAQUS, ANSYS, ADINA and many others [40-42].

In these programs, the computer simulates the behavior of physical systems using numerical modeling. which is a complex process involving several steps. Firstly, the physical model is developed by describing the physical system of interest in engineering terms. Next, a mathematical model is formed by translation of the physical model into a mathematical form. Then, we can construct the numerical model that can be solved using a computer, and which uses discretization methods such as the finite element method. Finally, the computer code is developed to simulate the behavior of the physical system.

3.2 Approximation with finite element modeling

To describe a domain, the approximation $u(x)$ can be used to obtain an approximate representation of a function that is difficult to evaluate, or known only at certain points and an approximation solution of an ordinary differential equation or partial differential equation [43]. When the domain becomes very larger, the number of nodes and parameters increases, thereby increasing the difficulty in the construction of an approximate function $u(x)$. Even more, complexity is introduced if the domain V has a complex shape and if the function of $u(x)$ must satisfy boundary conditions on the boundary of V [43].

The method of nodal approximation by subdomains was put forwarded in order to reduce the complexity and enable computer calculations. And this approach is the finite element approximation method, which is a particular type of approximation over subdomains with two characteristics. One is that the nodal approximation over each subdomain V^e depends only on the nodal variables attached to nodes located in V^e and on its boundary. The other one is that the approximate functions $u^e(x)$ over each subdomain V^e are constructed so as to be continuous over V^e and satisfy conditions of continuity between the different subdomains [44].

To define the geometry of a domain, a set of points is selected in the domain V and these points with the name of geometrical nodes might sometimes coincide with the interpolation nodes. Then, the domain V is replaced by a set of elements V^e, which has relatively simple shapes. Similarly, the subdomains should not overlap with each other by making distinct element have common points only their common boundaries. And there should not be any "holes" between elements.

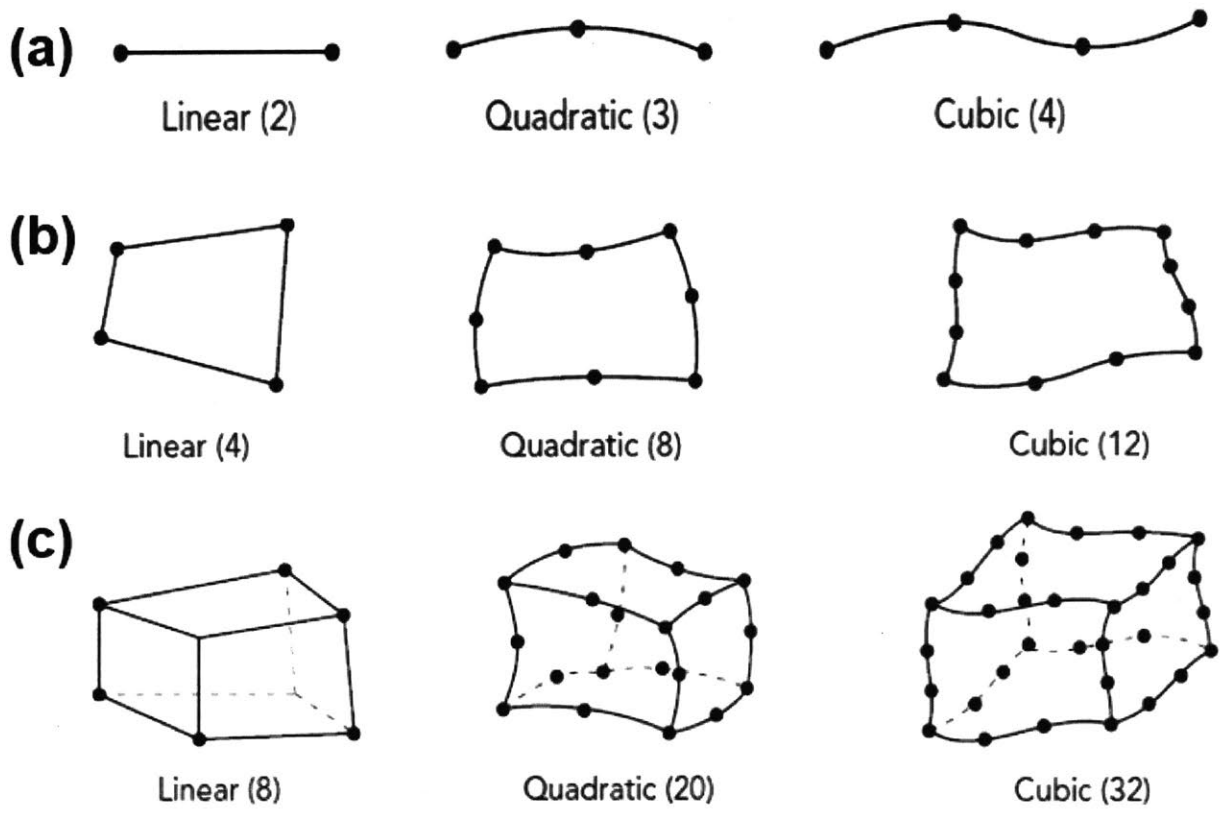

Figure 9 Common element shapes. (a-c) shows the one-, two- and three-dimensional elements distinctively. Reproduced with permission from Ref. [37]

Classical shapes for the elements can be categorized into one-, two- or three-dimensional elements. Each category has linear, quadratic and cubic elements as is shown in Figure 9. A reference element with regular and simple is introduced to simplify the analytical definition for elements of complex shapes and the reference may be transformed into any real element V^e by a geometrical transformation τ^e. In addition, a single reference element V^T maps into all the real elements V^e of the same type using different transformation τ^e (Figure 10) [45]. The transformation functions form a matrix for a system of elements and we can learn how the element deformed based on the transformation matrix. Deformation corresponds to stress field, which contains the axial stress and shear stress acting on the element along different directions. The information is very useful in various engineering analysis, such as structure analysis [37].

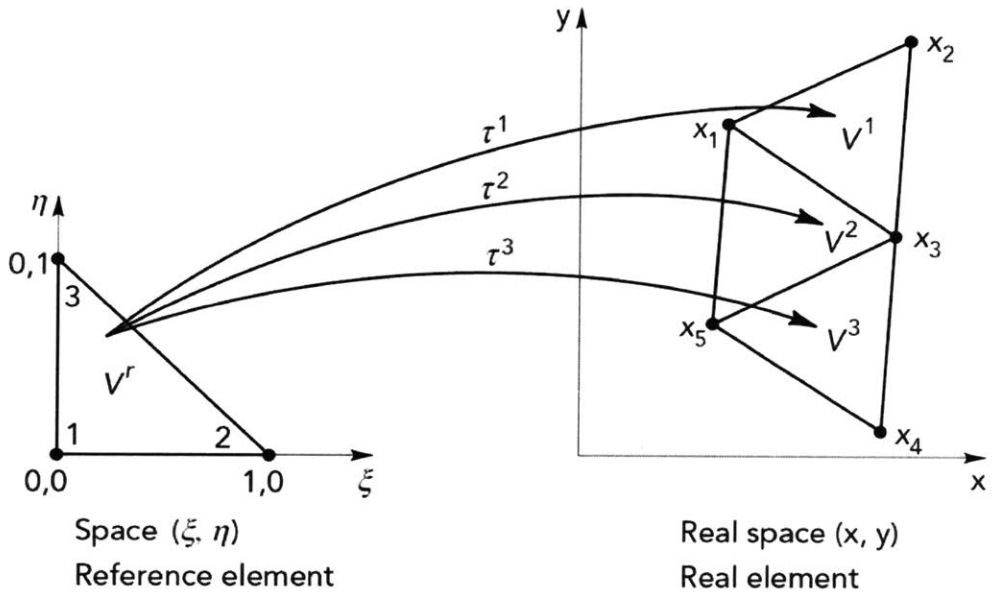

$$\text{Element 1}\quad \tau^1: \xi \rightarrow \mathbf{x}^1 = \mathbf{x}^1(\xi, \mathbf{x}_1, \mathbf{x}_3, \mathbf{x}_2)$$

$$\text{Element 2}\quad \tau^2: \xi \rightarrow \mathbf{x}^2 = \mathbf{x}^2(\xi, \mathbf{x}_1, \mathbf{x}_5, \mathbf{x}_3)$$

$$\text{Element 3}\quad \tau^3: \xi \rightarrow \mathbf{x}^3 = \mathbf{x}^3(\xi, \mathbf{x}_5, \mathbf{x}_4, \mathbf{x}_3)$$

Figure 10 Transformation from reference element to real element [37].

Chapter 4 Methodology

A series of computational bamboos are constructed. The effective material properties of bamboo unit cells with different proportions of fibers are determined by representative volume element (RVE) approach [46]. These properties are assigned to different regions in the complete bamboo computational models with different combinations of structural features. Finite element analysis is performed on the constructed models to measure the buckling resistance of various bamboo models.

4.1 Determination of effective material properties

4.1.1 Representative volume element (RVE) approach

A representative volume element (RVE) comprises the smallest portion of the composite that keeps the most representative combination of its main elements and materials [47]. The RVE approach is a very effective way to determine the properties of composite materials and improve the analysis efficiency by significantly reducing the computational cost [48]. The RVE can effectively capture different material structures by modifying the structures of the unit cells. Due to this, we can determine the effective material properties, i.e., engineering constant from different directions, by performing FEM analysis on these elements [49]. To calculate the effective stiffness tensor, iso-strain boundary conditions (ISBC) are applied on the representative domain to generate pure uniaxial stress and pure shear conditions.

4.1.2 Bamboo unit cells

As aforementioned, the mesoscale structure of bamboo cross section is heterogeneous and highly graded, with the population of longitudinal vascular bundles distributed non-uniformly through the wall thickness. The volumetric proportion of bamboo fiber increases approximately from 20% to 60% from the inner region to the outer region [3]. The exact values vary with different species. According to these material distribution patterns, the volumetric proportion of stiff fiber in the unit cells is assigned to be 20%, 30%, 40%, 50% and 60%. The formation and key design parameters

of the bamboo unit cell are shown in Figure 11. We design the unit cells with different fiber proportions by adjusting these design parameters according to the values listed in Table 1. The effect of fiber shape on the effective material properties is also taken into consideration by developing models with both circular and square fibers to make sure that effective material properties we obtained are consistent and shape independent. Mechanical properties of bamboo fiber and the surrounding matrix is very important for input for the unit cell. As previously mentioned, the elastic modulus of fiber and surrounding matrix are reported to be 55 GPa and 2 GPa separately [50]. In this research, the poison ratio of bamboo is taken as 0.35. Regarding the coordinating system, the fiber is considered to be continuous and oriented to the z axis (or in the direction 3 for the coordinate system 1-2-3) in the following FEM simulations.

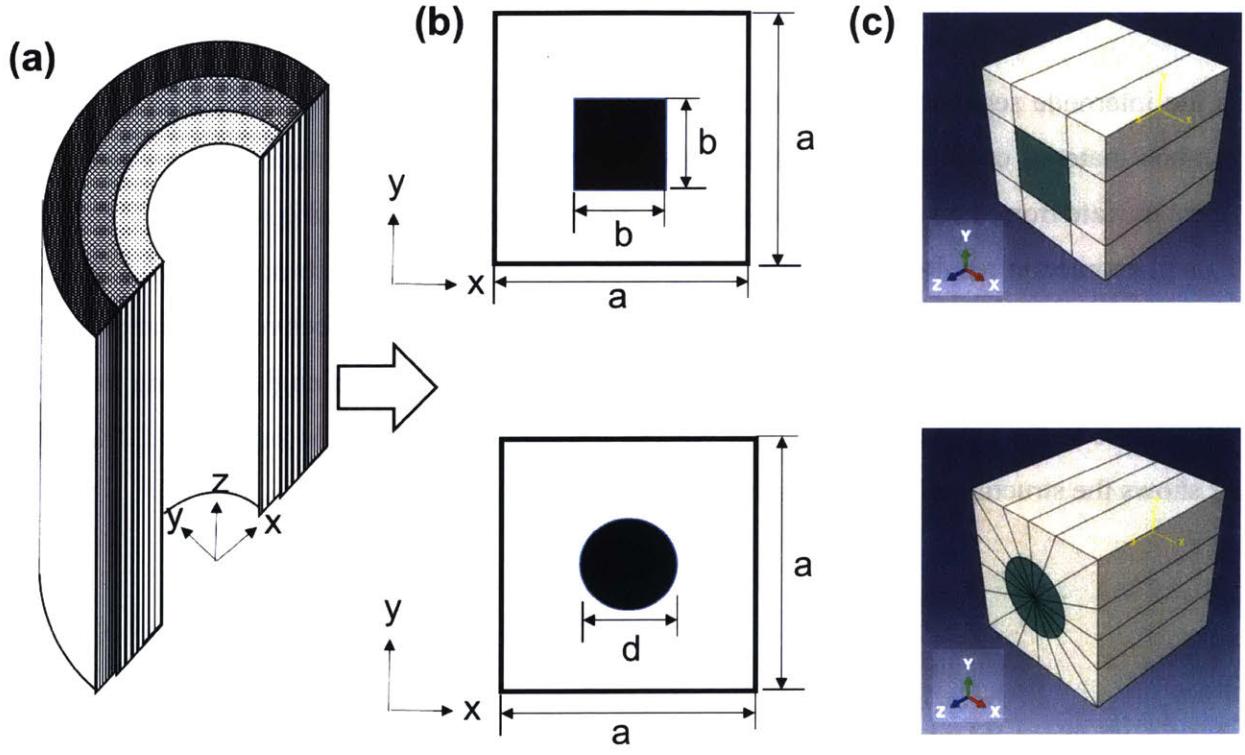

Figure 11 Structure of bamboo composite and its unit cells. (a) shows the fiber distribution density in the bamboo composite. Cubic unit cells taken out of the bamboo composite are shown in (b), where the upper and lower parts correspond to the square and circular fiber respectively. For the dimensional parameters, the side length of the unit cell is a. The side length of square fiber is b while the diameter of the circular fiber is d. The FEM models for both cases are displayed in (c), where fiber is in green while the surrounding matrix is in yellow.

Table 1 Summary of design parameters of bamboo unit cells (Unit: mm)

Fiber volumetric fraction	a	Fiber shape	
		b (Square)	d (Circular)
20%	10	4.5	5.1
30%	10	5.5	6.2
40%	10	6.3	7.1
50%	10	7.1	8.0
60%	10	7.7	8.7

In the internode segment, the orientation of bamboo fiber is strictly longitudinal so this part of bamboo material could be seen as transversely orthotropic composite material. By contrast, the fibers deviate from their original orientation at the vicinity of the node as is shown in Figure 2(b). This phenomenon results in the discrepancy in mechanical properties comparing with internode segment. It is necessary to investigate how fiber orientation affects effective material properties. Therefore, we develop a series of RVE with fibers inclined at different angles ranging from 0° to 90° relative to the z direction. The fiber volume fraction in these RVE is kept to be 20%. Figure 12 shows the structure of RVE with inclined fiber.

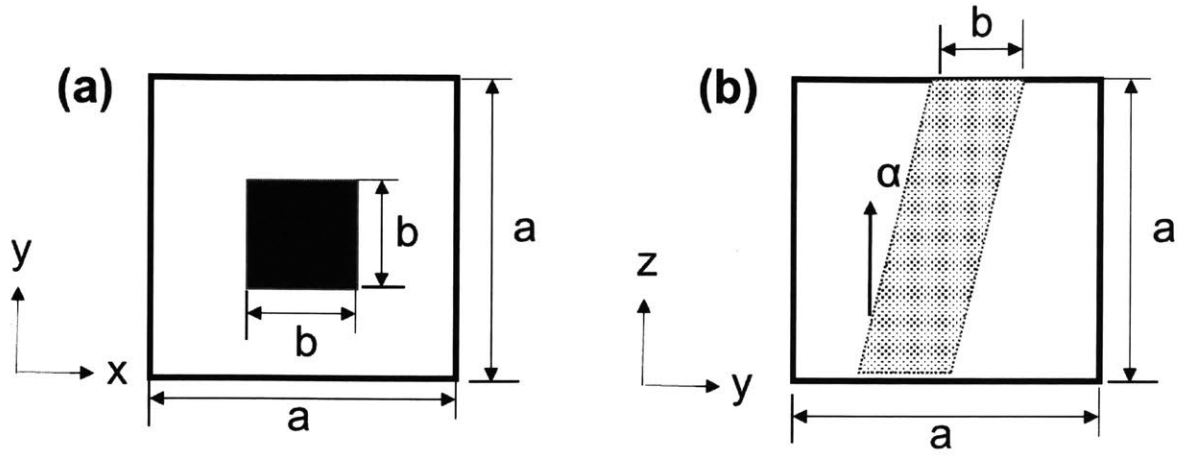

Figure 12 Representative volume element with inclined fiber. (a) View from the x-y plane. (b) View on the y-z plane. Angle α corresponds to angle formed between the fiber orientation and the longitudinal direction.

4.1.3 FEM on unit cells

We perform a series of finite element analysis with different boundary conditions with ABAQUS version 6.17 on these constructed bamboo unit cells. The simulation results could be used to obtain the effective material properties of the bamboo composite material. In terms of meshing, three-dimensional 20-node quadratic brick element (C3D20R) with displacement degrees of freedom (DOF) are used and the global sizing of the element is set to 1. We determine the independent coefficients in the constitutive relations in Equation (1) according to the stress and strain values obtained from FEM with different boundary conditions. Modeling the mechanical behavior of an RVE by its deformation can reflect its neighbor's behavior. Thus, in the simulations on unit cells, we apply iso-strain boundary conditions (ISBC), in terms of surface displacements, to the RVE to generate uniaxial stress and pure shear conditions. Spatial periodicity conditions are adopted in an RVE by making adjacent RVE have identical deformations. In this way, the compatibility demands with respect to opposite edges are satisfied and neither overlapping nor separation should occur. This compatibility condition is the so-called condition of parallelism.

More than one coefficient could be obtained for each analysis so only 6 analyses with different boundary conditions (Figure 12) are necessary for this research. For the determination of principal

moduli and Poisson's ratio (effective coefficients related to normal strain conditions), three separate analyses are performed by applying a unit displacement along three principal directions, i.e., positive x, y and z, distinctively. The normal displacement of all the other surfaces is set to 0. In all these 3 simulations, the values of normal stresses σ_{11}, σ_{22} and σ_{33} are recorded. Similar to this, in order to calculate the shear moduli (effective coefficients related to shear strain conditions), three separate analyses are performed by applying a unit displacement to generate shear strain along the positive xy, xz and yz directions respectively and the normal displacement on all the other surfaces are set to 0. This time, the values of shear stresses σ_{12}, σ_{23} and σ_{13} are recorded.

$$\begin{Bmatrix}\sigma_{11}\\ \sigma_{22}\\ \sigma_{33}\\ \sigma_{12}\\ \sigma_{23}\\ \sigma_{13}\end{Bmatrix} = \begin{bmatrix} c_{11}^E & c_{12}^E & c_{13}^E & 0 & 0 & 0 \\ c_{21}^E & c_{22}^E & c_{23}^E & 0 & 0 & 0 \\ c_{31}^E & c_{32}^E & c_{33}^E & 0 & 0 & 0 \\ 0 & 0 & 0 & c_{44}^E & 0 & 0 \\ 0 & 0 & 0 & 0 & c_{55}^E & 0 \\ 0 & 0 & 0 & 0 & 0 & c_{66}^E \end{bmatrix} \begin{Bmatrix}\varepsilon_{11}\\ \varepsilon_{22}\\ \varepsilon_{33}\\ \varepsilon_{12}\\ \varepsilon_{23}\\ \varepsilon_{13}\end{Bmatrix} \tag{1}$$

The compliance matrix (Equation 2) are derived after we achieved the effective coefficients in the constitutive relations by inverting the stiffness matrix. Then we can calculate our desired effective material properties, including the elastic modulus, shear modulus, and Poisson ratio, based on the compliance matrix.

$$\begin{Bmatrix}\varepsilon_{11}\\ \varepsilon_{22}\\ \varepsilon_{33}\\ \varepsilon_{12}\\ \varepsilon_{23}\\ \varepsilon_{13}\end{Bmatrix} = \begin{bmatrix} \frac{1}{E_1} & -\frac{\nu_{12}}{E_2} & -\frac{\nu_{13}}{E_3} & 0 & 0 & 0 \\ -\frac{\nu_{12}}{E_1} & \frac{1}{E_2} & -\frac{\nu_{31}}{E_3} & 0 & 0 & 0 \\ -\frac{\nu_{13}}{E_1} & -\frac{\nu_{23}}{E_2} & \frac{1}{E_3} & 0 & 0 & 0 \\ 0 & 0 & 0 & \frac{1}{2G_{12}} & 0 & 0 \\ 0 & 0 & 0 & 0 & \frac{1}{2G_{23}} & 0 \\ 0 & 0 & 0 & 0 & 0 & \frac{1}{2G_{13}} \end{bmatrix} \begin{Bmatrix}\sigma_{11}\\ \sigma_{22}\\ \sigma_{33}\\ \sigma_{12}\\ \sigma_{23}\\ \sigma_{13}\end{Bmatrix} \tag{2}$$

4.1.4 Effective material properties

The effective material properties for RVE with different fiber proportion and orientation are calculated by matrix orientation aforementioned. Table 2 summarizes the results for RVE of longitudinal fiber orientation while Table 3 summarizes the results for RVE of inclined fiber orientations. Moreover, the variation of elastic modulus along the longitudinal direction (E_3) with fiber orientation is plotted in Figure 13. It is interesting to note that the elastic modulus E_3 reduces by half when the fiber angle increase to 30° and the E_3 become a constant value when the relative angle exceeds 45°.

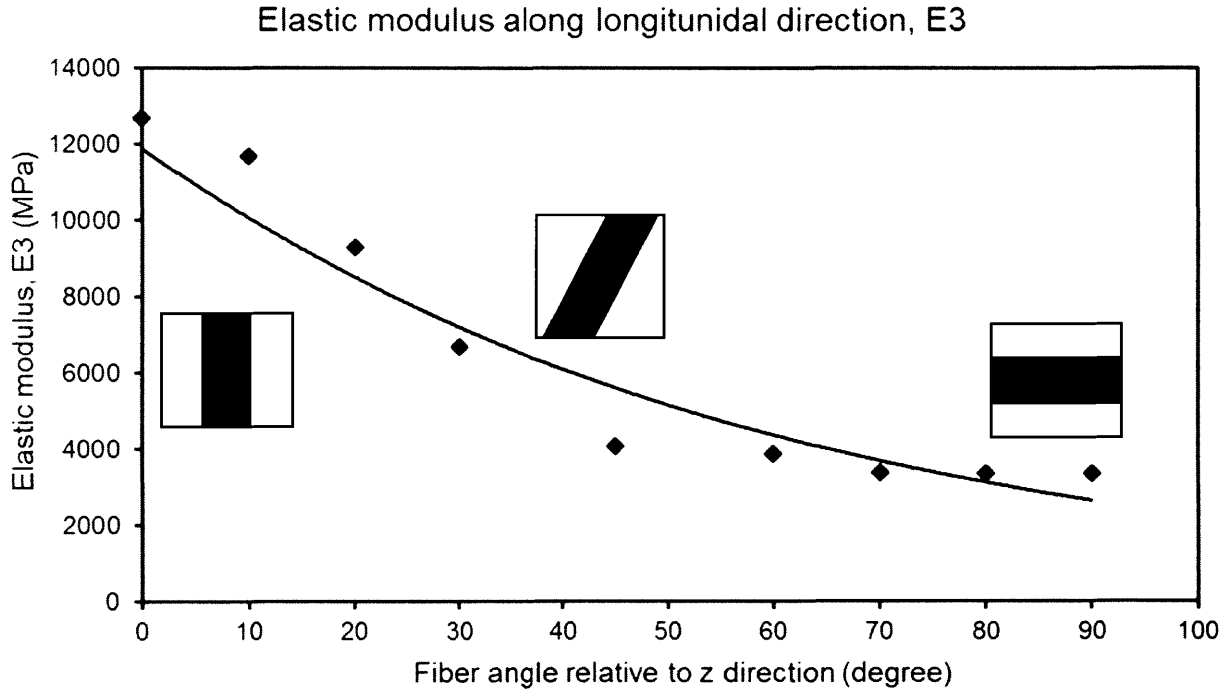

Figure 13 Variation of elastic modulus along the longitudinal direction (E_3) with respect to the fiber orientation.

Table 2 Engineering constants for RVE with fiber oriented along z direction

Engineering constants	Fiber volumetric fraction				
	20%	30%	40%	50%	60%
E_1(MPa)	3364.42	4309.37	5325.28	7043.47	10706.91
$E_2(MPa)$	3364.42	4309.37	5325.28	7043.47	10706.91
E_3(MPa)	12693.84	18032.50	22373.96	27970.01	36146.02
v_{12}	0.42	0.38	0.33	0.28	0.23
v_{13}	0.09	0.08	0.08	0.09	0.10
v_{23}	0.09	0.08	0.88	0.09	0.10
G_{12}(MPa)	1090.00	1328	1542.13	1928.56	2499
G_{13}(MPa)	2390.00	3689.12	4859.22	6470.82	8400
G_{23}(MPa)	2390.00	3689.12	4859.22	6470.82	8400

Table 3 Engineering constants for RVE with diverged fiber

Engineering constants	Fiber inclination								
	0°	10°	20°	30°	45°	60°	70°	80°	90°
E_1(MPa)	3364	3346	3371	3869	4066	6673	9292	11687	12693
E_2(MPa)	3364	3354	3407	3616	3742	3616	3407	3354	3364
E_3(MPa)	12693	11687	9292	6673	4066	3869	3371	3346	3364
v_{12}	0.42	0.41	0.39	0.30	0.19	0.10	0.10	0.09	0.09
v_{13}	0.09	0.11	0.17	0.37	0.60	0.37	0.17	0.11	0.09
v_{23}	0.09	0.09	0.10	0.10	0.18	0.30	0.39	0.41	0.42
G_{12}(MPa)	1090	1415	1730	2045	2385	1417	1732	2051	2390
G_{13}(MPa)	2390	1995	1730	1425	1087	1425	1730	1995	2390
G_{23}(MPa)	2390	2051	1732	1417	1090	2045	1730	1415	1090

4.2 Bamboo computational models

4.2.1 Multiscale structural features of bamboo models

After determining the effective material properties for different fiber volume fraction, we construct a series of bamboo computational models capturing structural features of bamboo. These models are used for further finite element analysis. For the bamboo fiber distribution density along the thickness direction of the bamboo cross section, previous studies divided the sections in into three regions, i.e., high fiber density, medium fiber density and low fiber density regions. Moreover, the average fiber volume fraction is reported to be approximately 40% and as previously mentioned, the fiber proportion varies from 20% to 60%. The fiber density could be reasonably estimated as 20%, 40% and 60% for the three regions respectively. This approximation is quite accurate because we observed similar proportion by analyzing the images of the bamboo cross section with ImageJ. Due to these reasons, in our FEA models, the bamboo cross section is divided into three layers with equal area. Their corresponding material properties are assigned to be the same with effective material properties of RVE with the fiber volume fraction of 20%, 40% and 60% from inner to outer periphery accordingly.

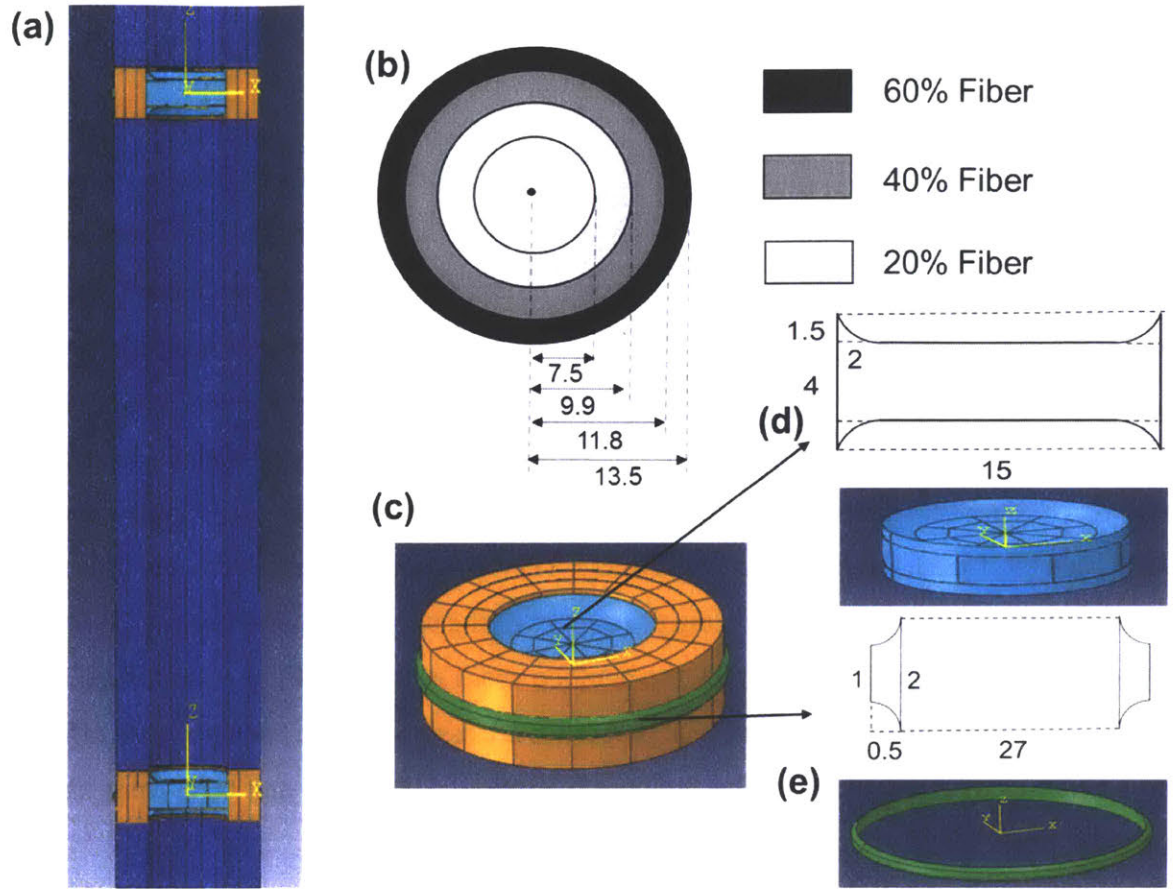

Figure 14 Multiscale structural features of bamboo computational models. (a) A vertical sectional view of bamboo model with all the structural features. (b) The cross section of bamboo with 3 layers of fiber distribution. (c) The structure of node with diverged fiber (yellow), internal diaphragm (blue) and external ridge (green). (d) The geometry of internal diaphragm. (e) The geometry of external ridge. (Unit: mm)

In terms of the macroscopic structure of bamboo along the longitudinal direction, bamboo segments are integrated by a series of regularly spaced nodes. The node structure includes an external ridge and internal diaphragm (Figure 14). As is shown in Figure 2(b), bamboo fibers change orientations at the vicinity of a node by deviating from their longitudinal culm direction. Furthermore, we can see that the elastic modulus along the longitudinal direction (E_3) decreases sharply when the fiber slightly deviates from the culm direction and the value reduces by half when the inclination reaches about 30°, followed by a constant value of E_3 when the inclination exceeds

45°. Thus, the elastic constants of materials at the node is assigned to be half the value of the culm at the same thickness layer in order to accurately simulate the fiber divergence. Material properties at the external ridge are set to be identical with those of the outermost layer while the material properties at the internal diaphragm are assigned to be the same with the innermost layer. In this way, we can maintain consistency within our FEA model. Moreover, we assign the geometry and dimension of these two structural features by measuring and analyzing real bamboo samples so that we can make sure that our computational model design is realistic.

4.2.2 Critical length estimation

In order to study the buckling behavior of bamboo, it is necessary to ensure that buckling dominates the failure of bamboo computational models. For simplicity, the cross-section of bamboo is assumed to have a uniform fiber distribution of 40% and the bamboo model is pin connected at the both boundaries. The critical buckling load can be evaluated by Equation (3).

$$P_{cr} = \frac{\pi^2 EI}{L^2} \tag{3}$$

And the load causing bamboo model to fail by crushing can be calculated by Equation (4).

$$P_y = \sigma_y A \tag{4}$$

The bamboo model fails by buckling if $P_{cr} < P_y$, meaning that the critical length of bamboo model should be calculated in Equation (5).

$$L_{cr} = \pi \sqrt{\frac{EI}{\sigma_y A}} \tag{5}$$

By plugging in the values of each variable, the critical length of the bamboo model is roughly estimated to be 160mm. However, we did not take into account of the macroscale structural features so the total length of our bamboo model is set to be 500mm in order to ensure the failure mode is buckling.

4.2.3 Computational models with different feature combinations

To make an accurate model, we measure the dimensions of several samples. The average inner and outer diameters are measured to be 7.5 mm and 13.5 mm respectively. The average segment length is 100 mm by measurement.

Our research objective is to study the effect of each structural feature on the compressive strength of bamboo. To achieve this goal, we construct a series of bamboo models by assembling the macroscopic structural features in several combinations. To study the effect of fiber deviation at the node, we construct a bamboo model in a hollow tube form with continuous fiber and several bamboo models with periodic weak connections between segments with a certain length. To investigate and compare the contribution from the ridge and diaphragm, we add the following features to the models with periodic weak connections: external ridge only, internal diaphragm only, and both external ridge and internal diaphragm. To test how these effects mentioned above vary with segment length, we assign each type of model with the segment length of 20mm, 40mm, 50mm, 60mm, 80mm, 100mm, 120mm, and 140mm.

4.3 Boundary conditions of FEM on complete bamboo models

Finite element analysis has been performed on these completed bamboo models with ABAQUS/Standard. Three-dimensional 20-node quadratic brick with reduced integration (C3D20R) is used to mesh the models. The global sizing of mesh element in the tubular portion is set to be 3 while the global sizing in the structural features (internal diaphragm and external ridge) is set to be 1.5. The analysis is carried out by the method of linear perturbation. As is shown in Figure 15, the load is applied at one end along the longitudinal direction. In terms of boundary conditions, the model is pinned at the loaded end and fixed at the unloaded end (Figure 15). Eigenvalues and buckling shapes for the first 5 buckling modes are recorded for further analysis. The critical buckling load can be calculated by multiplying the Eigen-values with the area.

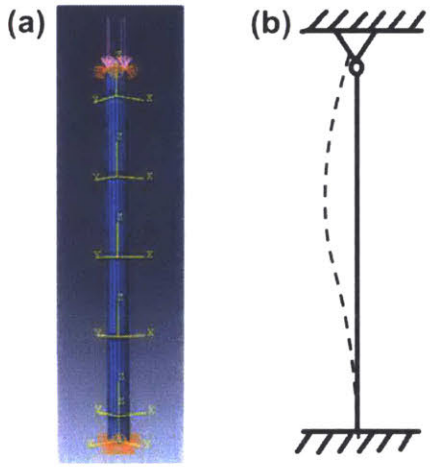

Figure 15 Boundary conditions for bamboo models. (a) shows the boundary conditions and load application on the bamboo models. (b) shows the theoretical graph of a column pinned at the top and fixed at the bottom, which is equivalent to our settings. The dashed line is the buckling shape.

Chapter 5 Results

This section summarizes the analytical calculation on fiber distribution and an analysis of the simulation results. The effect of multiscale structural features is interpreted based on the result analysis.

5.1 Fiber distribution pattern on bending stiffness of bamboo

By theory, the critical buckling load for a column is estimated by Equation (6),

$$P_{cr} = \frac{\pi^2 EI}{(kL)^3}. \tag{6}$$

The term kL is the effective length of the column. The value is totally dependent on the boundary conditions. For FEM simulations with the same boundary condition, the compressive strength is only dependent on the flexural rigidity (EI), which is related to the cross sectional properties of the column. In terms of the bamboo cross section (Figure 16a), the fiber distribution along the thickness is divided into three regions from outer periphery to inner periphery: high fiber density (60%), medium fiber density (40%) and low fiber density (20%). To prove the advantage of such fiber distribution pattern in maximizing the flexural rigidity, we calculated the flexural rigidity of two other cases. The first one (Figure 16b) demonstrates the uniform fiber distribution (40%) throughout the cross section and the second one (Figure 16c) also demonstrates a three-layer pattern like bamboo but in a reverse order. The flexural rigidity of the three cross sections are calculated by Equation (7),

$$EI = E_i I_i = E_1 I_1 + E_2 I_2 + E_3 I_3 \tag{7}$$

where $E_i I_i$ is the flexural rigidity for each layer. The value of E is taken as the corresponding elastic modulus along the longitudinal direction (E_3). Though the total amount of fiber are the same, the calculated $E_i I_i$ values vary significantly. As is shown in Figure 16, the flexural rigidity results for the three cases are $6.29 \times 10^8\ N \cdot mm^2, 5.28 \times 10^8\ N \cdot mm^2$ and $4.93 \times 10^8\ N \cdot mm^2$ respectively. By comparing these values, it is noted that the fiber distribution pattern of the

bamboo cross section could almost increase 20% of the compressive strength comparing to the uniformly distributed case. However, the reverse distribution pattern decreases the compressive strength by 20%. Thus, the fiber distribution pattern within bamboo cross section is optimized to provide a maximized flexural rigidity, leading to a maximized critical load of buckling.

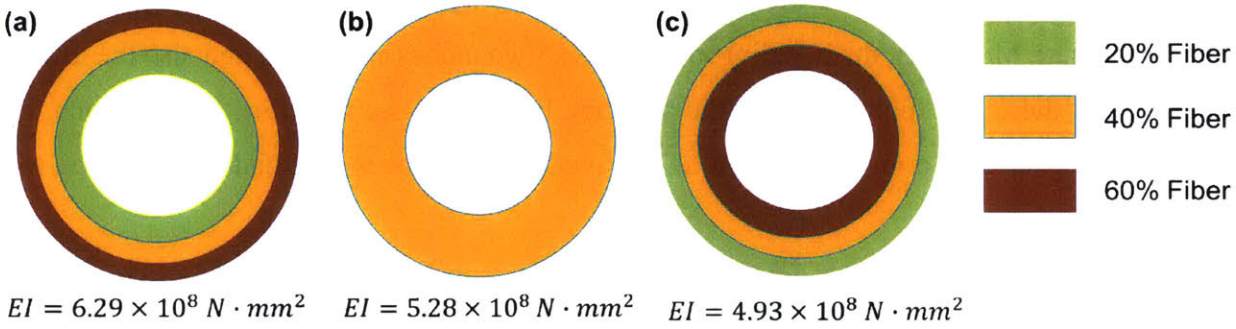

Figure 16 Three types of fiber distribution pattern. (a) shows the bamboo fiber density distribution. (b) shows the uniform fiber distribution. (c) shows the reverse of bamboo fiber density distribution.

5.2 Finite element modeling results

5.2.1 Critical buckling shapes

The buckling shapes of the first five buckling modes are shown in Figure 17. We notice that the first two buckling modes have the identical shape but the only different is the bending directions are perpendicular. Moreover, the buckling load for these two modes are similar and also the lowest, indicating that these two modes control the buckling behavior. As a result of these reasons, the critical buckling load of a model is taken as the average of the buckling loads for the first two modes.

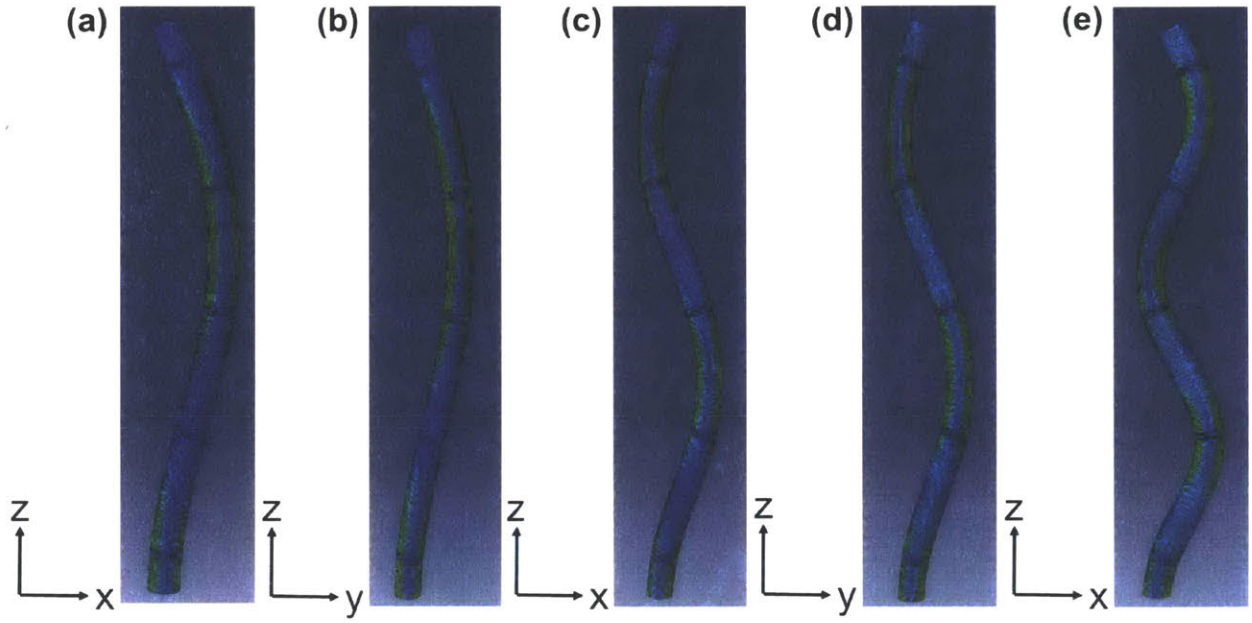

Figure 17 Buckling shapes for the first five buckling modes. Panels (a-e) correspond to the first to fifth buckling modes respectively.

5.2.2 Critical buckling loads

Based on the finite element analysis results, the critical load of buckling for the bamboo model with continuous fiber is estimated as 51.82 kN. The analytical solution of the buckling load is calculated by Equation (6). Regarding the effective length kL, the factor k is theoretically proved to be 0.7 according to the boundary conditions shown in Figure 15b and the flexural rigidity is

$6.29 \times 10^8\ N \cdot mm^2$. Thus, the value of analytical solution is computed to be 51.64 kN, which is consistent with the FEM results within allowable limits of error. In order to make sure that this consistency is independent with the length, we also performed finite element analysis on the models with the length of 400mm and 600mm. The results from FEM and theoretical calculation agree reasonably well, revealing that our computational models and FEM settings are suitable. The critical buckling loads for the all the models with various combinations of structural features are summarized in Table 4 and further analysis are made based on these results.

Table 4 Critical buckling load for bamboo models (Unit: kN)

Features / Segment length	Diverged fiber	Internal diaphragm	External ridge	Ridge and diaphragm
20mm	37.29	37.54	37.65	37.90
40mm	43.16	43.32	43.40	43.57
50mm	44.87	45.01	45.08	45.24
60mm	45.49	45.59	45.67	45.78
80mm	46.75	46.86	46.91	47.02
100mm	48.10	48.20	48.22	48.32
120mm	48.07	48.15	48.19	48.27
140mm	48.80	48.88	48.90	48.98

5.3 Fiber divergence

5.3.1 Result analysis

As mentioned previously, bamboo fiber starts to diverge from its original longitudinal direction at the vicinity of nodes. To study how fiber divergence at the node affect the buckling behavior, we plotted the critical buckling load values against segment lengths in Figure 18. Comparing with the continuous fiber model, the models connected by diverged fiber (weak connection) have a much lower critical loading force, ranging from only 75% to 95%. Moreover, as the segment length increases, it is noted that the critical buckling load gradually increases before the segment length reaches 100mm. After the segment length exceeds 100mm, the value of critical buckling load plateaued. This set of data is also analyzed by fitting a curve with the exponential form,

$$P_{cr,weak} = P_{cr,0} - A \times e^{\left(-\frac{L}{L_0}\right)} = 51.82 - 18.46 \times e^{\left(-\frac{L}{60}\right)}. \quad (8)$$

It matches very well with the simulation data and the parameter 60 indicates the minimum segment length that the critical load starts to be steady. Obviously, for a bamboo model with given length, larger segment length means fewer weak connections in the model.

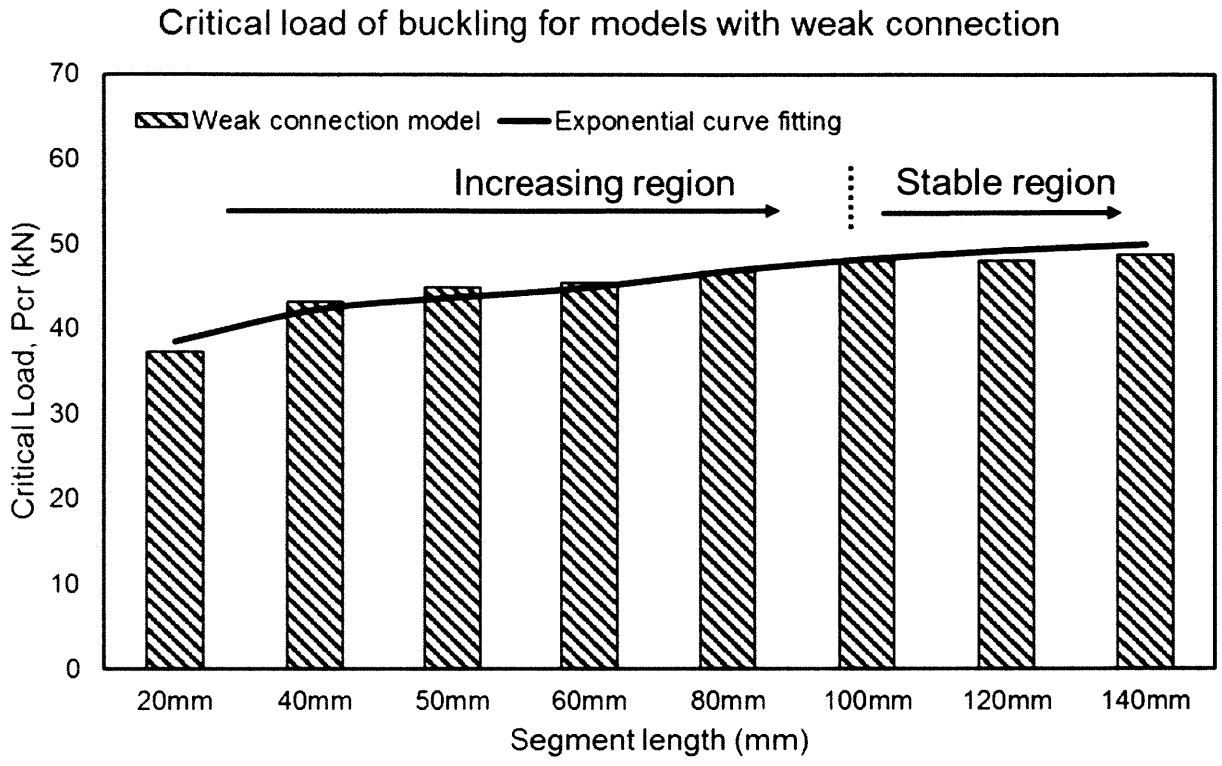

Figure 18 Critical buckling load for models connected with diverged fiber. The horizontal axis shows the segment length while the vertical axis demonstrates the value of critical buckling load from FEM. The values are fitted to an exponential expression, which is shown by the continuous line.

5.3.2 Effect of fiber divergence

According to this information, we find that the presence of fiber divergence at the node decreases the elastic modulus along the longitudinal direction (E_3), resulting in the reduction of buckling resistance for bamboo model. The reduction effect recedes when there are fewer weak connections and becomes nearly constant when the segment length is large enough. Therefore, to achieve a relatively large critical buckling load, the segment length should be large enough but after reaching the steady region, further increase segment length may not be that helpful.

5.4 External ridge and internal diaphragm

5.4.1 Result analysis

In addition to the diverged fiber, there are also two structural features at the node, namely internal diaphragm and external ridge. In order to investigate how these two features contribute to the buckling resistance, we plotted the critical buckling loads of models with either internal diaphragm or external ridge against segment lengths in Figure 19 and Figure 20. In terms of the critical buckling load, both of the two models shows a similar trend as the model connected by diverged fiber: increase with segment length followed by a relatively stable value. In addition to critical buckling load, we calculated the additional load the model could carry, defined by Equation 9, in order to highlight the reinforcing effect from these structural features.

$$P_{add} = P_{cr} - P_{cr,weak} \tag{9}$$

5.4.2 Effect of external ridge and internal diaphragm

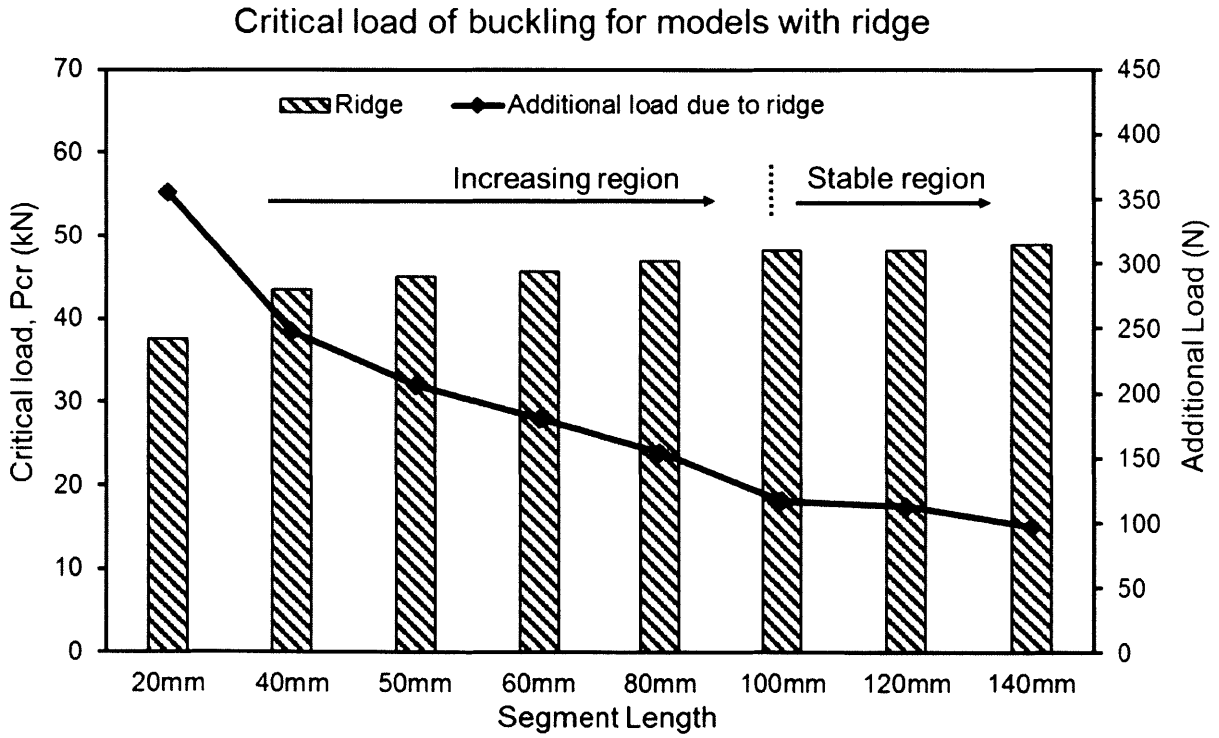

Figure 19 Critical buckling load and additional load contributed by an external ridge.

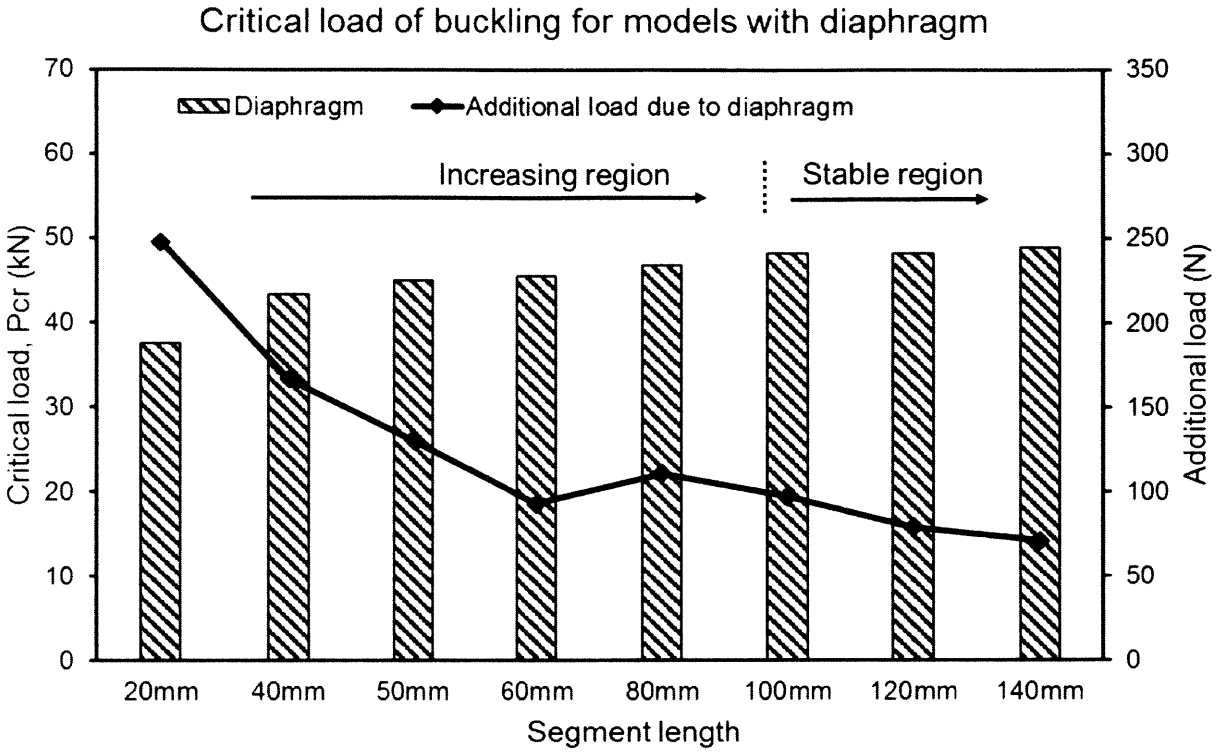

Figure 20 Critical buckling load and additional load contributed by internal diaphragm.

As is shown in Figure 19 and Figure 20, the additional load significantly descends before the segment length reaches the value of 100 mm and following that, the contribution from structural features plateaued because there are a fewer external ridge or internal diaphragm in the model as the segment length increases.

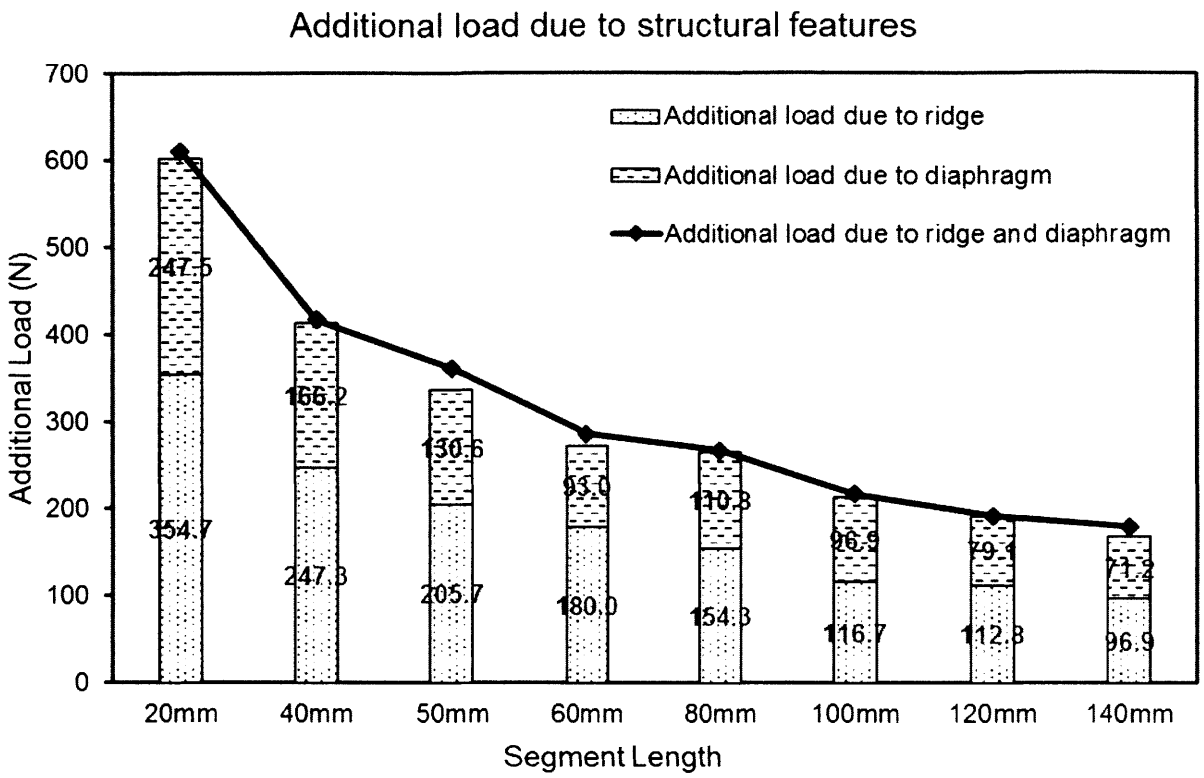

Figure 21 Additional load due to the presence of different combinations of macroscopic structural features on the node.

In order to compare the effectiveness of these two features and investigate if there is a bonus effect when they present together, we plotted the additional load due to different combinations of these structural features in Figure 21. From the data on the chart, we could notice that the contribution from the external ridge is 36% to 55% more than that from the internal diaphragm. Nevertheless, based on the dimension shown in Figure 14, the volume of external ridge is computed to be 52.5 mm^3, which is only about $\frac{1}{16}$ of the volume of internal diaphragm (838.8 mm^3). Therefore, external ridge is much more effective and efficient in generating the reinforcing effect than internal diaphragm.

In addition, the total height of the stacking bar chart represents the summation of the reinforcing effect due to individual structural features. The data point on the line chart shows the additional load the model could carry when both the structural features present together. It is noted that the

value on the line chart is roughly the same with the total additional loads, revealing that the reinforcing effect from the internal diaphragm and external ridge could be directly added up together but there is no extra collaborative effect. As a result, the changing trend of the total addition load also demonstrates a falling downtrend until the segment length is larger than 100mm. Even though the contribution from structural features is more significant when the segment length is shorter, the total load capacity, critical buckling load, of the model with the longer segment is higher. Overall speaking, the segment length should be large enough to gain higher critical buckling load.

Chapter 6 Discussions

In this section, we present the explanation for regular segment length, cross-species comparison, innovative applications of bamboo and inspiration for the biomimetic design.

6.1 Explanation for regular segment length

The segments on the bamboo culm are periodically connected by nodes and the segment length is roughly a constant value. From the biological perspective, the nodes play a significant role in the growth of bamboo. They provide places for branches and leaves, which provide nutrients for bamboo by photosynthesis. Moreover, meristems, which trigger the growth of new cells, are located at every node. In this way, every bamboo segment could grow simultaneously, resulting in the rapidly growing rate of the plant. Therefore, the nodes are favorable and indispensable for bamboo to grow. From the structural mechanics' perspective, the distance between neighboring nodes determines both the weakening effect from fiber divergence and strengthening effect from the internal ridge and external diaphragm. In our case, when the segment length exceeds 100mm, both the detrimental result and beneficial result become stable value but not very significant. However, a balance is achieved because a relatively higher compressive strength is obtained, meaning the overall buckling performance of the completed bamboo structure is optimized. The critical segment length value relies on the cross-sectional properties and it is computed to be 100mm for our case. Furthermore, the average segment length of our real bamboo samples approximately equals to 231mm with the standard deviation of 35mm by measurement and this value is far beyond 100mm. Therefore, when choosing structural bamboo, we should select the ones with segment length over the critical value to obtain optimized mechanical performance.

6.2 Cross-species comparison

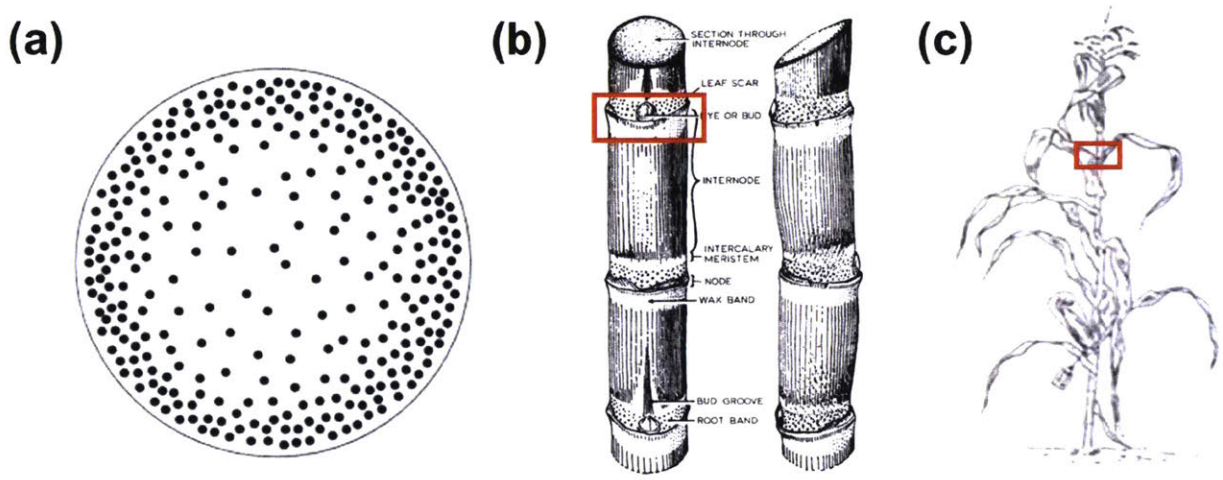

Figure 22 Other species with similar structural features. (a) Cross section of a palm tree with gradient fiber distribution pattern. Reproduced with permission from Ref [51]. (b) shows the stem of sugar cane. Reproduced with permission from Ref [52]. (c) shows the stem of corn respectively. Reproduced with permission from Ref [53]. Both of sugar cane and corn have a periodic external ridge.

Interestingly, other species also developed these favorable structural features, such as the fiber distribution pattern, external ridge, and internal diaphragm, in the evolutionary process, revealing the effectiveness and universality of these features. In the mesoscale, the cross section of a palm tree, shown in Figure 22(a), demonstrates a similar gradient fiber distribution pattern with bamboo: dense fiber near the outer periphery but sparse in the center. This pattern is optimized to give the maximized compressive strength. In the macroscale, the stems of sugar cane (Figure 22b) and corn (Figure 22c) also have periodic external ridges, which contribute to the buckling resistance of these plants as well. It is noted that sugar cane has almost the same exterior appearance with bamboo and the only distinction lies in the interior section: bamboo culm is tubular but sugar cane stem is solid. Thus, this difference logically brings about a question that whether the external ridge on sugar cane is as useful as on bamboo, leading the necessity to quantitatively compare the contributions. Based on the finite element analysis on sugar cane and bamboo models (with the

same cross-sectional flexural rigidity), the additional buckling load is plotted against the segment length in Figure 23 for apparent comparison. We notice that the presence of external ridge could also strengthen the buckling resistance of the sugar cane but the additional load due to the external ridge of the tubular cross section is slightly more significant than that of solid cross section. Therefore, the external ridge is a little bit more useful for tubular structures similar to bamboo.

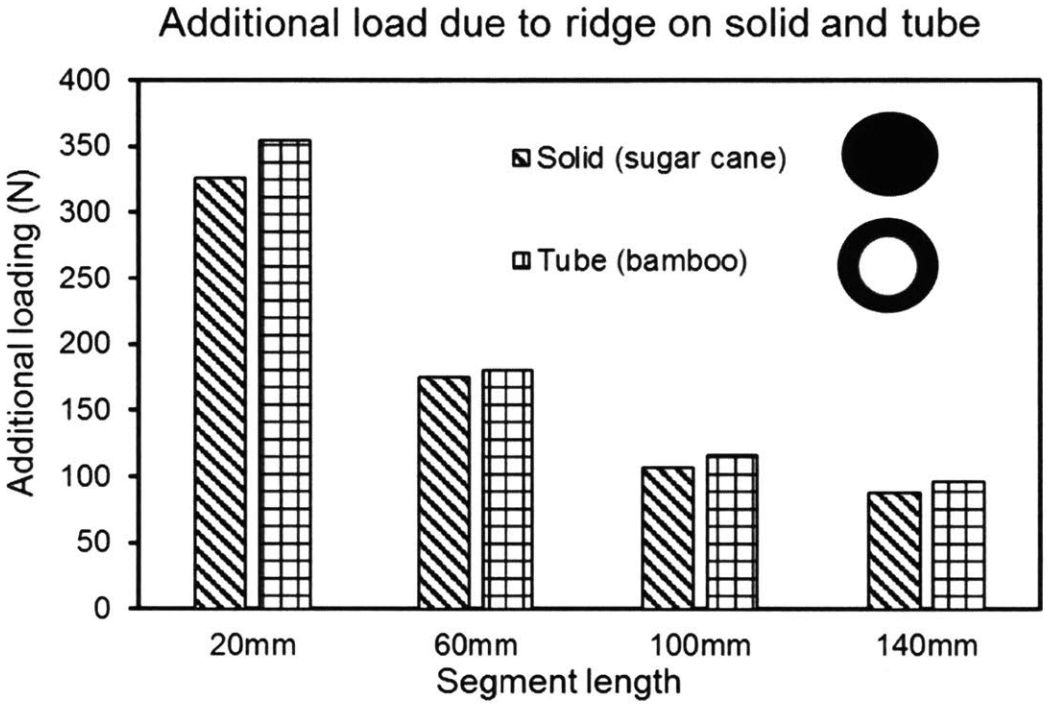

Figure 23 Comparison between sugar cane and bamboo. This figure shows how the additional load due to the external ridge on sugar cane model and bamboo model change with the segment length.

6.3 Innovative applications of bamboo

Characterized as an intelligent natural composite material with optimized fiber distribution, bamboo could be given many promising applications because of its maximized compressive strength[51]. In the structural engineering field, a high-volume of bamboo is used as building and scaffolding material, acting as the alternative for steel tubing [54]. Our research result is very helpful for structure engineers to perform better bamboo column design to avoid dreadful buckling failure mode. In the materials engineering field, bamboo fibers could serve the reinforcing function for composite materials to achieve excellent mechanical properties [55, 56]. In the musical field, bamboo could be made into flutes, soundboards, xylophone bars and many other percussion instruments, by making use of its effective sound radiation resulted from the high bending stiffness at low density [33]. In the sports field, bamboo culm is an excellent material for making pole-vaulting poles owing to its strength and elastic energy storage per unit weight [57]. The promotion of these applications would mitigate the pressures on the ever-shrinking natural forest, bring down the growing demand for carbon steel, facilitate the conservation of the global environment and achieve the sustainable development purpose.

6.4 Inspiration for biomimetic design

The naturally adapted multiscale structure of bamboo could be taken as a reference in bio-inspired or biomimetic design in many ways, providing us with advanced materials and structures. For material design, we are inspired to develop synthetic composite materials with gradations using bamboo cross section as a template for emulation. For structural member design, structural features, such as the internal diaphragm and external ridge, could be equipped with columns in compressive loading for improving the buckling resistance as well as decorating. For structural system designs, the working principle of mechanical floors in skyscrapers are very similar to the internal diaphragm and similarly, the ring-like structure seen in bamboo may also be added to skyscrapers for further stabilizing buildings by mimicking the more efficient external ridge.

Chapter 7 Conclusion

7.1 Summary of major findings

In this research, the effects of multiscale structural features – gradient fiber distribution and periodic nodes – on the critical buckling load of bamboo were studied systematically. We determined the effective material properties of the composite structure by performing finite element analysis on representative volume elements, constructed by considering the volumetric proportion, orientation and shape of bamboo fibers. We developed a series of computational models to systematically investigate the role of the structural features on which FEA simulations are performed to obtain critical buckling load. Our results show that the heterogeneous fiber distribution has a great advantage to amplify the flexural rigidity by 20% comparing to the uniform fiber distribution, resulting in the significant enhancement of the buckling resistance of bamboo. We determined that the function of nodes is favorable and indispensable to provide a place for leaves to grow, but from a structural point of view, the presence of nodes actually weakens the buckling resistance of bamboo because of the fiber deviation at the vicinity of nodes. We have identified that other structural features including external ridge and internal diaphragm can both reinforce bamboo against buckling and external ridge is found to play a more significant role than the internal diaphragm. For bamboo with roughly the same cross-sectional properties as our samples, the segment length of 100mm is a critical value partitioning the entire bamboo by inserting nodes, as longer segment length will not yield significantly larger critical buckling load. This important result agrees well with the average segment length of our real bamboo samples by measurement. The exact critical value is dependent on the cross-sectional properties. Some of these favorable structural features on bamboo are also developed in other species such as palm tree, sugar cane and corn, which may also explain their regular internode distance for this mechanical perspective.

7.2 Impact of research results

Our findings could inspire us to create innovative composite materials, columns, and even superstructure forms by bio-mimicking these beneficial structural features in bamboo.

In composite material design, we can manipulate the distribution pattern of the stiff and soft component in order to achieve a smart composite material with tunable mechanical properties. In structural column design, we can adopt a hollow tube form so that materials are distributed further away than solid column, thereby increasing the buckling resistance and providing a space for installing drainage pipes and building services. We can also introduce the external ridge feature onto structural columns to enhance the buckling resistance and achieve aesthetic architecture. In high-rise superstructure design, we can insert several very stiff mechanical floors along the height of the building, which serves the function similar to the internal diaphragm in bamboo.

Our research may also contribute to achieve sustainable development purpose by inventing more innovative application of bamboo.

In current construction industry, the usage of structural steel is very common but the embodied carbon coefficient of steel is nearly 20 times of that of bamboo. Replacing steel with bamboo in some construction projects will not only significantly reduces the carbon dioxide emission but also decrease the material cost. Moreover, our forest resource is ever-shrinking and it is non-renewable because of the extremely low growth rate of wood. Replacing timber with bamboo can help us to mitigate the shortage of non-renewable materials.

Therefore, the research results can contribute to the innovative design, economy development and environmental protection.

7.3 Future work

Our computational models are limited to the demonstrating the mechanical performance of bamboo at the mesoscale and macro-scale. However, the structure-property relationship of bamboo fiber at a molecular level remains unanswered. In addition, apart from the cellulose and water, there are also some minerals in bamboo, such as silica dioxide. But we have no idea about the function of mineralization from the mechanical point of view. Answering these problems are, however, beyond the scope of this study.

Future studies could set up atomistic models to establish an understanding of molecular features of bamboo. Molecular dynamics and other multiscale simulation approaches may be performed to understand the mechanical behavior of the composite bamboo material and function of each chemical component from the atomistic scale upwards.

Chapter 8 References

[1] B. Hameed, A. M. Din, and A. Ahmad, "Adsorption of methylene blue onto bamboo-based activated carbon: kinetics and equilibrium studies," *Journal of hazardous materials,* vol. 141, pp. 819-825, 2007.

[2] Z. Ben-Zhi, F. Mao-Yi, X. Jin-Zhong, Y. Xiao-Sheng, and L. Zheng-Cai, "Ecological functions of bamboo forest: research and application," *Journal of Forestry Research,* vol. 16, pp. 143-147, 2005.

[3] T. Tan, N. Rahbar, S. Allameh, S. Kwofie, D. Dissmore, K. Ghavami, and W. Soboyejo, "Mechanical properties of functionally graded hierarchical bamboo structures," *Acta biomaterialia,* vol. 7, pp. 3796-3803, 2011.

[4] T. Y. Lo, H. Cui, and H. Leung, "The effect of fiber density on strength capacity of bamboo," *Materials Letters,* vol. 58, pp. 2595-2598, 2004.

[5] X. Song, G. Zhou, H. Jiang, S. Yu, J. Fu, W. Li, W. Wang, Z. Ma, and C. Peng, "Carbon sequestration by Chinese bamboo forests and their ecological benefits: assessment of potential, problems, and future challenges," *Environmental Reviews,* vol. 19, pp. 418-428, 2011.

[6] Z. J. Zhai and J. M. Previtali, "Ancient vernacular architecture: characteristics categorization and energy performance evaluation," *Energy and Buildings,* vol. 42, pp. 357-365, 2010.

[7] M. Sarkisian, E. Long, C. Doo, and D. Shook, "Natural structural systems and forms," in *AEI 2011: Building Integration Solutions*, ed, 2011, pp. 188-195.

[8] A. R. Prasad and K. M. Rao, "Mechanical properties of natural fibre reinforced polyester composites: Jowar, sisal and bamboo," *Materials & Design,* vol. 32, pp. 4658-4663, 2011.

[9] S. Lakkad and J. Patel, "Mechanical properties of bamboo, a natural composite," *Fibre Science and Technology,* vol. 14, pp. 319-322, 1981.

[10] D. Fang, S. Wu, F. K. Wong, and Q. Shen, "A comparative study on safety and use of bamboo and metal scaffolding in Hong Kong," *Construction Safety Management Systems,* p. 340, 2004.

[11] H. Lingard and S. Rowlinson, "Behavior-based safety management in Hong Kong's construction industry," *Journal of Safety Research,* vol. 28, pp. 243-256, 1998.

Chapter 8 References

[12] K. Chung and W. Yu, "Mechanical properties of structural bamboo for bamboo scaffoldings," *Engineering Structures,* vol. 24, pp. 429-442, 2002.

[13] H. Kefu and M. Bingyang, "Growth of Bamboo Shoots and the Young Bamboo of Phyllostachys makinoi," *JOURNAL OF FUJIAN COLLEGE OF FORESTRY,* p. 04, 1994.

[14] S. I. Yamamoto, N. Nishimura, and K. Matsui, "Natural disturbance and tree species coexistence in an old-growth beech-dwarf bamboo forest, southwestern Japan," *Journal of Vegetation Science,* vol. 6, pp. 875-886, 1995.

[15] K. Takahashi, S. Uemura, J. I. Suzuki, and T. Hara, "Effects of understory dwarf bamboo on soil water and the growth of overstory trees in a dense secondary Betula ermanii forest, northern Japan," *Ecological Research,* vol. 18, pp. 767-774, 2003.

[16] D. C. Franklin and D. M. Bowman, "A multi-scale biogeographical analysis of Bambusa arnhemica, a bamboo from monsoonal northern Australia," *Journal of Biogeography,* vol. 31, pp. 1335-1353, 2004.

[17] D. Taylor, B. Kinane, C. Sweeney, D. Sweetnam, P. O'Reilly, and K. Duan, "The biomechanics of bamboo: investigating the role of the nodes," *Wood Science and Technology,* vol. 49, pp. 345-357, 2015.

[18] W. Liese, "Research on bamboo," *Wood Science and Technology,* vol. 21, pp. 189-209, 1987.

[19] R. Kappel, C. Mattheck, K. Bethge, and I. Tesari, "Bamboo as a composite structure and its mechanical failure behaviour," *WIT Transactions on Ecology and the Environment,* vol. 73, 2004.

[20] L. Osorio, E. Trujillo, A. Van Vuure, and I. Verpoest, "Morphological aspects and mechanical properties of single bamboo fibers and flexural characterization of bamboo/epoxy composites," *Journal of Reinforced Plastics and Composites,* vol. 30, pp. 396-408, 2011.

[21] L. Zou, H. Jin, W.-Y. Lu, and X. Li, "Nanoscale structural and mechanical characterization of the cell wall of bamboo fibers," *Materials Science and Engineering: C,* vol. 29, pp. 1375-1379, 2009.

[22] S. Youssefian and N. Rahbar, "Molecular origin of strength and stiffness in bamboo fibrils," *Scientific reports,* vol. 5, 2015.

Chapter 8 References

[23] F. Libonati and M. J. Buehler, "Advanced Structural Materials by Bioinspiration," *Advanced Engineering Materials,* 2017.

[24] S. Amada and S. Untao, "Fracture properties of bamboo," *Composites Part B: Engineering,* vol. 32, pp. 451-459, 2001.

[25] K. Okubo, T. Fujii, and Y. Yamamoto, "Development of bamboo-based polymer composites and their mechanical properties," *Composites Part A: Applied science and manufacturing,* vol. 35, pp. 377-383, 2004.

[26] M. E. Lewis, *Construction of Space in Early China, The*: SUNY Press, 2012.

[27] H. Z. L. C. W. Yan and G. Beide, "Application of Bamboo Materials in Civil Construction [J]," *Forest Engineering,* vol. 2, p. 027, 2007.

[28] F. Albermani, G. Goh, and S. Chan, "Lightweight bamboo double layer grid system," *Engineering Structures,* vol. 29, pp. 1499-1506, 2007.

[29] G. Minke, *Building with Bamboo: Design and Technology of a Sustainable Architecture*: Walter de Gruyter, 2012.

[30] M. Yee, "Engineered bamboo furniture with mortise and tenon joints," ed: Google Patents, 2006.

[31] J. Atanda, "Environmental impacts of bamboo as a substitute constructional material in Nigeria," *Case Studies in Construction Materials,* vol. 3, pp. 33-39, 2015.

[32] S. BORAN, A. DÖNMEZ ÇAVDAR, and M. C. BARBU, "Evaluation of bamboo as furniture material and its furniture designs," *Pro Ligno,* vol. 9, 2013.

[33] U. G. Wegst, "Bamboo and wood in musical instruments," *Annu. Rev. Mater. Res.,* vol. 38, pp. 323-349, 2008.

[34] W. Yu, K. Chung, and S. Chan, "Column buckling of structural bamboo," *Engineering Structures,* vol. 25, pp. 755-768, 2003.

[35] J. Porteous and A. Kermani, *Structural timber design to Eurocode 5*: John Wiley & Sons, 2013.

[36] P. Code, "Eurocode 3: Design of Steel Structures-Part 1-2: General Rules-Structural Fire Design," 2007.

[37] G. Dhatt, E. Lefrançois, and G. Touzot, *Finite element method*: John Wiley & Sons, 2012.

[38] K. J. Bathe, *Finite element method*: Wiley Online Library, 2008.

Chapter 8 References

[39] K.-J. Bathe and E. L. Wilson, *Numerical methods in finite element analysis* vol. 197: Prentice-Hall Englewood Cliffs, NJ, 1976.

[40] A. U. Manual, "Version 6.10," *ABAQUS Inc,* 2010.

[41] A. Fluent, "12.0," *Theory guide,* 2009.

[42] Y.-c. XIONG and Y.-g. FANG, "Secondary development of material constitutive model in ADINA software," *Rock and Soil Mechanics,* vol. 29, pp. 2221-2225, 2008.

[43] T. J. Hughes, *The finite element method: linear static and dynamic finite element analysis*: Courier Corporation, 2012.

[44] J. N. Reddy, *An introduction to the finite element method* vol. 2: McGraw-Hill New York, 1993.

[45] J. Dolbow and T. Belytschko, "A finite element method for crack growth without remeshing," *International journal for numerical methods in engineering,* vol. 46, pp. 131-150, 1999.

[46] R. d. Medeiros, M. E. Moreno, F. D. Marques, and V. Tita, "Effective properties evaluation for smart composite materials," *Journal of the Brazilian Society of Mechanical Sciences and Engineering,* vol. 34, pp. 362-370, 2012.

[47] T. Kanit, S. Forest, I. Galliet, V. Mounoury, and D. Jeulin, "Determination of the size of the representative volume element for random composites: statistical and numerical approach," *International Journal of solids and structures,* vol. 40, pp. 3647-3679, 2003.

[48] W. Drugan and J. Willis, "A micromechanics-based nonlocal constitutive equation and estimates of representative volume element size for elastic composites," *Journal of the Mechanics and Physics of Solids,* vol. 44, pp. 497-524, 1996.

[49] C. Sun and R. Vaidya, "Prediction of composite properties from a representative volume element," *Composites Science and Technology,* vol. 56, pp. 171-179, 1996.

[50] S. Amada, "Hierarchical functionally gradient structures of bamboo, barley, and corn," *Mrs Bulletin,* vol. 20, pp. 35-36, 1995.

[51] U. G. Wegst, "Bending efficiency through property gradients in bamboo, palm, and wood-based composites," *Journal of the mechanical behavior of biomedical materials,* vol. 4, pp. 744-755, 2011.

[52] R. P. Humbert, *The growing of sugar cane*: Elsevier, 2013.

Chapter 8 References

[53] P. C. Mangelsdorf, *Corn. Its origin, evolution and improvement*: Belknap Press of Harvard University Press, 1974.

[54] T. Sen and H. J. Reddy, "Application of sisal, bamboo, coir and jute natural composites in structural upgradation," *International Journal of Innovation, Management and Technology,* vol. 2, p. 186, 2011.

[55] H. Takagi and Y. Ichihara, "Effect of fiber length on mechanical properties of "green" composites using a starch-based resin and short bamboo fibers," *JSME International Journal Series A Solid Mechanics and Material Engineering,* vol. 47, pp. 551-555, 2004.

[56] Y. Mi, X. Chen, and Q. Guo, "Bamboo fiber-reinforced polypropylene composites: Crystallization and interfacial morphology," *Journal of applied polymer science,* vol. 64, pp. 1267-1273, 1997.

[57] N. P. Linthorne, "Energy loss in the pole vault take-off and the advantage of the flexible pole," *Sports Engineering,* vol. 3, pp. 205-218, 2000.